CHAPTER 8

OXYGEN SPECIES

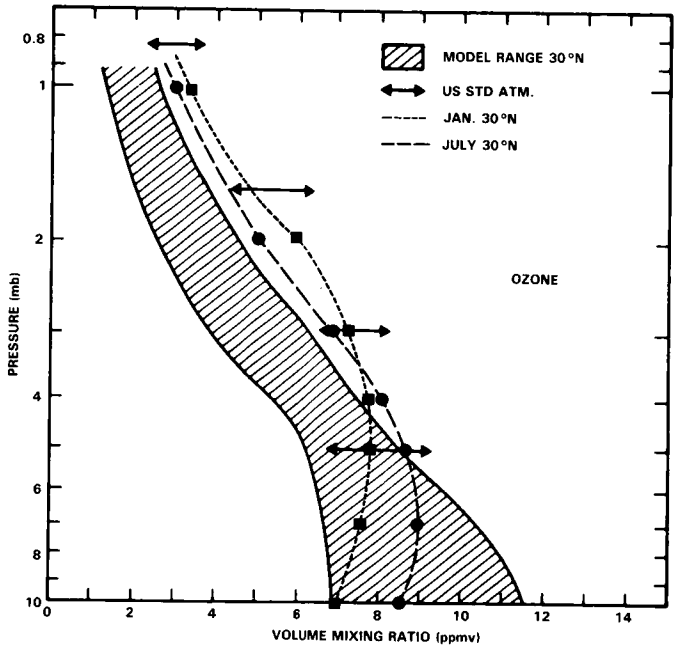

Panel Members

G. Brasseur and A.J. Miller, Co-Chairmen

P.K. Bhartia
A. Fleig
L. Froidevaux
D. Heath
E. Hilsenrath
J.A. Logan
P. McCormick
G. Megie
R. Nagatani
J.M. Russell, III
R.J. Thomas

CHAPTER 8

OXYGEN SPECIES: OBSERVATIONS AND INTERPRETATION

TABLE OF CONTENTS

8.0 INTRODUCTION

The problems related to odd oxygen (O_3, O and $O(^1D)$) in the atmosphere and especially to ozone (O_3) have been extensively discussed in the last 10-20 years. Ozone is indeed the only atmospheric constituent which effectively absorbs ultraviolet solar radiation from about 250 to 310 nm, protecting plant and animal life from exposure to harmful radiation (UV-B). Moreover, since the absorbed solar energy is converted into thermal energy, the absorption of UV light by ozone constitutes the principal source of heat in the middle atmosphere and is therefore responsible for the existence of the stratosphere, a layer with a positive temperature gradient and a considerable static stability.

The possible long-term decrease in the ozone amount is therefore expected not only to increase the UV-B irradiance at the earth's surface, but also to modify the thermal structure or the atmosphere with potential consequences on the general circulation and on the global and local climate of the Earth.

As indicated previously in Chapter 2, stratospheric and mesospheric ozone is produced by photodissociation of molecular oxygen

$$O_2 + h\nu \rightarrow O + O \tag{1}$$

followed by a three-body recombination reaction

$$O + O_2 + M \rightarrow O_3 + M \tag{2}$$

Its destruction can occur by recombination with atomic oxygen

$$O + O_3 \rightarrow 2O_2 \tag{3}$$

This reaction, however, can be catalyzed by a number of atmospheric species such as the pairs of radicals OH and HO_2, NO and NO_2, or Cl and ClO. A representative picture of the height-dependent percent contribution of these cycles to the odd oxygen loss at mid-latitudes is shown in Figure 8-1. The direct recombination (Chapman, 1930) plays its major role near the stratopause while the effect of nitrogen (Crutzen, 1970), which is the globally dominant ozone loss occurs essentially in the middle and lower stratosphere. Destruction by hydrogen compounds dominates in the mesosphere, at low altitude in the troposphere and near the tropopause. Chlorine plays a significant role (and will play an even larger role in the future) in the upper stratosphere.

The ozone balance is thus controlled on the one hand by the solar irradiance and its penetration into the denser layers of the atmosphere and on the other hand by the atmospheric abundance or species involved in the O_x, HO_x, NO_x and ClO_x systems. These chemical families will be considered in detail in the next three chapters.

The purpose of this chapter is to determine how the spatial distribution of ozone, as predicted by numerical models, compares with observations. Since numerical predictions of the future ozone trend are based on models which make use of this complex chemistry, it is important to state how well we understand that chemistry and what are the possible sources of discrepancies between models and observations. Toward this, we will develop a set of reference ozone profiles against which to compare current numerical calculations.

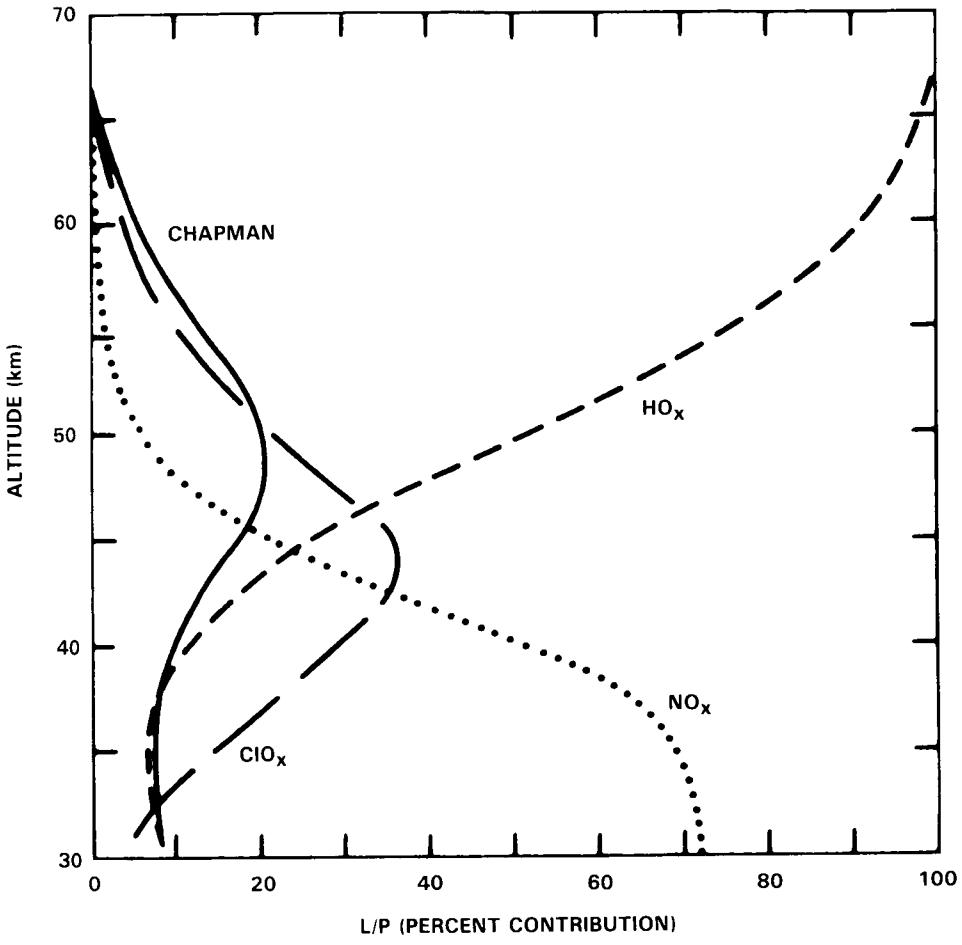

Figure 8-1. Ratio (in percent) of the odd oxygen loss rate due to the Chapman, HO_x, NO_x, ClO_x mechanisms to the odd oxygen production rate (based on mid-latitude diurnal average calculation with the Caltech 1-D model; JPL 1985 recommended photochemical data). L and P are the O_x loss and production rates respectively.

The comparison between measured and calculated ozone distributions is not always straightforward. Indeed, below about 25 km, the photochemical lifetime of odd oxygen is long compared to the characteristic time for meridional and vertical transport. In the lower stratosphere, the ozone distribution is thus heavily influenced by dynamics and the large ozone variability which is observed reflects effects due to advection, large scale planetary waves, turbulence, etc. In the upper stratosphere and in the mesosphere, ozone can more easily be used to test our present knowledge of the chemistry since the chemical lifetime of odd oxygen is short and the direct influence of transport processes is weak. Figure 8-2, taken from the 2-D model of Garcia and Solomon (1985), shows the O_x photochemical lifetime as a function of altitude and the resulting regions of dynamical and chemical control. Most of the analyses reported in the present chapter will focus on ozone between 30 and 70 km altitude. Even in this region, however, transport processes can influence the ozone distribution, in particular at high latitudes during the winter and spring seasons, when large scale planetary waves and stratospheric warmings occur. In an attempt to isolate the photochemical effects, one should therefore also try to avoid the above regions, unless one can track a certain air parcel and analyze the ozone changes within it, as they relate to temperature or other observable chemical changes.

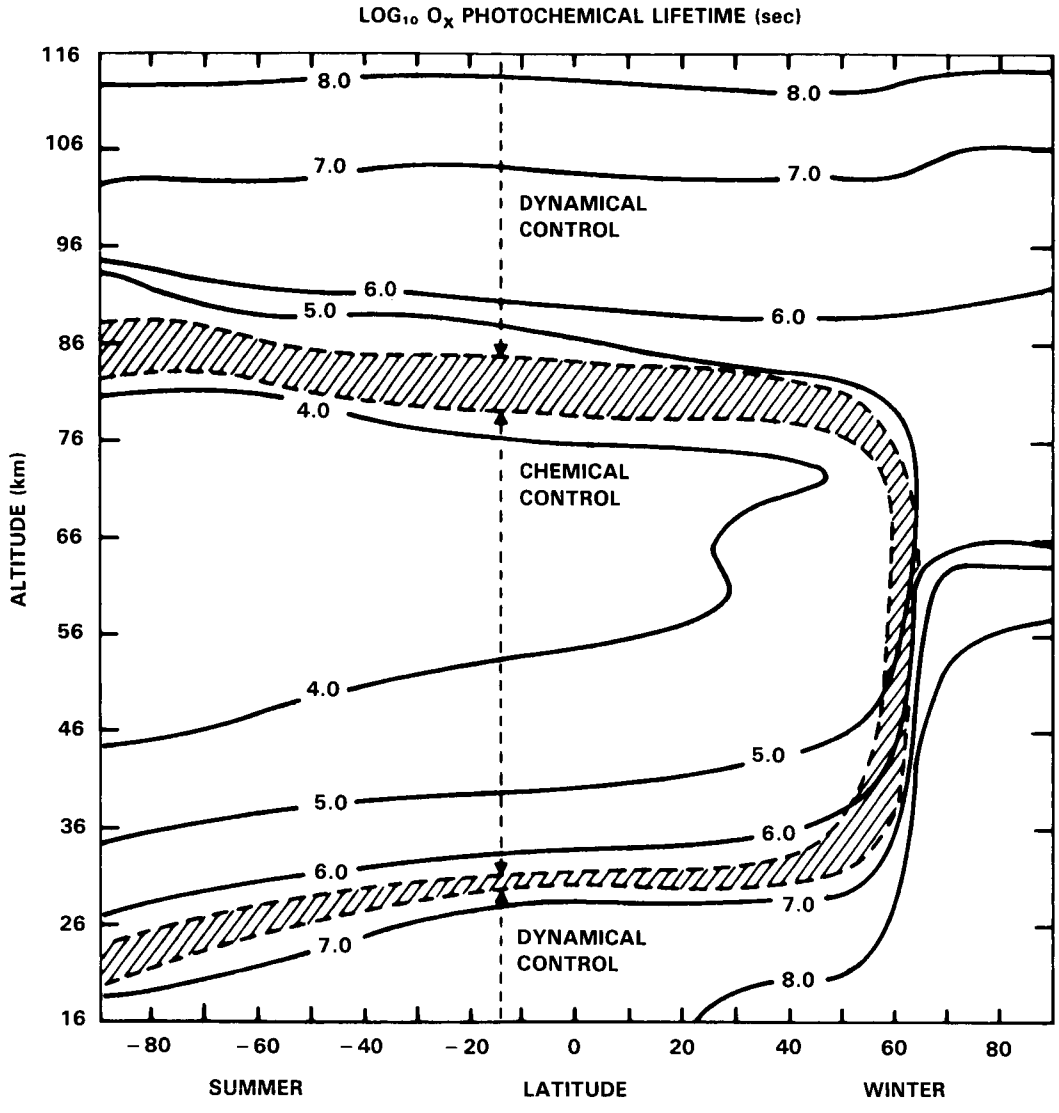

Figure 8-2. Photochemical lifetime of the O_x family and the region of transition from photochemical to dynamical control (shaded) (From Garcia and Solomon, 1985).

8.1 OZONE REFERENCE PROFILES

Our approach within this section is to utilize recent satellite observations as well as ground-based data to provide the necessary global coverage. Because the Solar Backscatter Ultraviolet (SBUV) instrument, launched in 1978, provides the longest data record of the satellite systems, we focus on these data as the basic system. A major feature of this section, however, is a discussion of the comparison of SBUV versus LIMS, SAGE and SME satellite systems as well as the ground-based observations to provide evidence of the absolute accuracy of the profiles. This, combined with the estimates of sampling errors and year-to-year variations provides the basic confidence estimates of the observations for the model comparisons.

8.1.1 Instruments

8.1.1.1 Satellite Systems

General descriptions of the satellite systems are described above such that within this section we will focus on the error analyses pertinent to our understanding of the random and absolute error characteristics.

The operating characteristics of the SBUV system are presented in Tables 8-1 and 8-2 (Bhartia, personal communication) where Table 8-1 pertains to time invariant errors and Table 8-2 the random error component. We see that at 1 mbar the combined time-invariant error is about 7% and decreases to about 3% for total ozone. For the random error component the combined error is about 5% except at the upper end of the profile data where it increases to 10%.

Table 8-1. Nimbus-7 SBUV Systematic Error Summary (Bhartia and Fleig, Personal Communication).

Error Source	Ozone Mixing Ratio Error (%) .4 mb	1 mb	3 mb	10 mb	30 mb	Total Ozone
1. Ozone absorption cross-section	3	3	3	3	3	3
2. Wavelength calibration	0.5	0.5	0.6	0.7	0.7	0.7
3. Radiometric calibration	7	5	3	2	2	1
4. Retrieval error	10	3	2	4	5	1
RSS of (1) thru (4)	13	7	5	5	6	3

Notes: a) Values are maximum possible error (1 σ confidence) from each error source in mid latitudes
b) Error 1 applies only for SBUV comparisons with non-UV instruments. Within Ultraviolet errors should be less than 1%.
c) Errors 1 and 4 should be ignored in comparing similar SBUV instruments on different satellites.

Total ozone measurements made by the SBUV have been compared with those from over 60 Dobson stations (Bhartia *et al.*, 1984a). The result is that SBUV is lower, on average, by about 8% and the standard deviation of the differences is consistent with the estimates of about 2% precision on each instrument type.

With respect to comparisons of SBUV profiles, Bhartia *et al.* (1984b) have compared the results with Umkehr and balloon ozonesonde information. The biases are generally less than 10%, but are functions of layer height and latitude. The precision of the SBUV measurements is found to be better than 8% from pressures between 1 and 64 mbar and better than 15% from 64 to 253 mbar.

The biases between SBUV and the ground-based observations, discussed above, are believed to be largely due to inconsistencies in the ozone absorption cross sections used for the various measurement systems. This is currently being reexamined utilizing new absorption coefficients derived by Bass and

Table 8-2. Nimbus-7 SBUV Random Error Summary (Bhartia and Fleig, Personal Communication).

Error Source	Ozone Mixing Ratio Error (%) .4 mb	1 mb	3 mb	10 mb	30 mb	Total Ozone
1. Instrument noise	2	1	1	2	2	0.5
2. Atmospheric temp	1	0.5	1	1	1	1
3. Retrieval error	10	3	2	4	5	2
RSS of (1) thru (3)	10	3	2.5	5	5	2

Notes: a) Errors listed are R.M.S. values for typical mid latitude measurements. During winter months or under disturbed atmospheric conditions. Errors 2 and 3 may be larger by a factor of 2.
b) Vertical resolution of SBUV derived profiles is ~8 km. Resolution related limitations are not included.

Paur (personal communication) and recently recommended by the International Ozone Commission for use in the satellite retrievals.

For the LIMS experiment, details of the preflight calibration are presented by Gille and Russell (1984). Within Table 8-3 are presented the LIMS systematic errors (Remsberg *et al.*, 1984a) and we see that the errors are about 20% save at the lower and upper end of the profiles where they increase to 40%. The authors note that the random ozone radiometric errors are about equal to the systematic radiometric errors from 30 to 0.3 mbar.

An extensive program of correlative balloon underflights was carried out to aid in validation of LIMS data. The results of the correlative measurement comparisons, accuracy calculations, and precision estimates are presented by Remsberg *et al.*, 1984a. Comparisons with sets of correlative ozone profiles show mean differences of less than 10% from 7 to 50 mbar for mid-latitude balloon borne sensors and 16% from 0.3 to 50 mbar for rocket data. Such results are well within the uncertainties for the correlative sensors themselves. Agreement with balloon measurements degrades somewhat at tropical latitudes in the lower stratosphere. LIMS detects significant vertical structure in the ozone profile even below the ozone mixing ratio peak. Preliminary comparisons with Umkehr data at four stations show generally good agreement from 1 to 30 mbar.

Results of comparison between SAGE and ground-based data have been summarized by McCormick *et al.* (1984) for 5 sets during 1979-1980. The intercomparisons included data taken with electrochemical ozone (ECC) balloonsondes and chemiluminescent and optical rocketsondes. The average mean difference for 17 separate comparisons between the SAGE and ECC balloonsonde observations over the altitudes 18-28 km was 9.3% with a standard deviation of 2.8%. Excluding comparisons separated by greater than 500 km reduces the average mean difference to 8.9% and the standard deviation to 2.1%. The average mean difference between SAGE and three optical rocketsonde observations over the altitudes 25-50 km was 11% and between SAGE and two chemiluminescent rocketsondes over the altitudes 20-60 km was 13.5%. Considering the differences in vertical resolution, experimental errors, and ozone time and space

gradients, the agreement between SAGE-derived ozone profiles and these correlative measurements is considered very good. In addition, isopleths of ozone mixing ratio versus latitude and altitude are in good agreement with previously published results.

Within Tables 8-4 and 8-5 are presented the systematic and random error components, respectively. We see that the systematic component is about 2.5% and the random component is of the order of 10% except at the highest level where it is 40%. This value, however, is a worst case scenario for 1 km resolution.

Rusch *et al.* (1984) have examined the error characteristics of the SME experiment and in Table 8-6 and 8-7 we reproduce their results for the systematic and random components, respectively. We see that the systematic errors are about 16% over the entire range, while the random errors are about 6% at 48 km increasing to about 14% at 68 km.

Table 8-3. LIMS O_3 Channel Systematic Error Sensitivity Results.

Error Parameter	O_3 Mixing Ratio Error, %						
	100 mb	30 mb	10 mb	3 mb	1 mb	0.3 mb	0.1 mb
1. Systematic radiometric errors*	5	2	1	1	2	5	20
2. Temperature profile bias (±2 K)	34	32	20	12	10	12	12
3. O_3 spectral parameters	15	12	10	8	8	8	8
4. IFOV side lobes	14	2	2	3	6	20	31
5. Deconvolution error	5	5	5	5	5	5	5
6. rss of rows 1-5	40	35	23	16	15	26	40

* Random O_3 radiometric errors are about equal to the systematic radiometric errors from 30 to 0.3 mbar.

Table 8-4. SAGE Ozone Systematic Error Summary (McCormick and Chu, Personal Communication).

Error Source	1 mb	7 mb	50 mb	100 mb	Total Ozone
1. Ozone absorption cross-section	1.5%	1.5%	1.5%	1.5%	1.5%
2. Wavelength calibration	2.0%	2.0%	2.0%	2.0%	2.0%
3. Rayleigh correction	0.5%	0.5%	0.5%	0.5%	0.5%
	2.5%	2.5%	2.5%	2.5%	2.5%

Table 8-5. SAGE Ozone Random Error Summary (McCormick and Chu, Personal Communication).

Error Source	1 mb	7 mb	50 mb	100 mb	Total Ozone
1. Measurement noise	40%	5%	10%	10%	1.0%
2. Atmospheric temperature	0.3%	0.2%	0.2%	0.5%	0.2%
3. Aerosol correction	0	0	1.0%	2%	0.5%
4. Tropospheric ozone	0	0	0	0	1%
	40%	5%	10.1%	10.2%	1.5%

Notes: a) Error 1 applies only when SAGE data are used at 1 km altitude resolution. Error magnitude can be reduced by vertical averaging giving an improvement factor of $\sqrt{N}$, where N is the number of km altitude being averaged; i.e., the 10% error at 50 mb can be reduced to approximately 3.3% when 10 km vertical averaging is done.

b) SAGE ozone profiles begin at cloud top altitude. Total ozone is determined using climatology mean for the tropospheric ozone component.

8.1.1.2 Ground-Based Systems

As the ground-based data systems (except for the recent LIDAR results) have been extensively discussed in the recent reports of Hudson and Reed (1979) and WMO (1982), we will present here only a brief overview and update as required.

8.1.1.3 Total Ozone

The most widely used tool for monitoring total ozone continues to be the Dobson ozone spectrophotometer. This instrument is a quartz-prism double-monochromator, which measures the differential attenuation of sunlight in adjacent spectral bands in the UV Huggins bands of ozone. By use of a double wavelength pair method with direct sunlight, measurements precise to $\pm 2\%$ are possible. Empirical relationships between measurements on direct sunlight and zenith skylight have been derived. This allows a less accurate estimation of total ozone on partly cloudy and cloudy days.

In the U.S.S.R., a filter photometer system, the M-83, is used for total ozone measurements. In a direct comparison with the Dobson spectrophotometer, Bojkov (1969) found differences as large as 40 percent. These differences, which depend on the solar zenith angle and the season, apparently arise from the use of broadband filters and the assumption of constant ozone absorption coefficients. The U.S.S.R. has about 35 M-83 instrument reporting stations. Error estimates of the Dobson system are presented by Hudson and Reed (1979). We note, however, that this table does not take into consideration the recently derived ozone absorption coefficients of Bass and Paur.

It should be noted here that Dobson spectrophotometers are no longer being produced. A. W. Brewer has developed a grating ozone spectrophotometer which is now available commercially. Preliminary evaluation indicates that the Brewer instrument provides direct sun total ozone observations of precision comparable to the Dobson (Kerr *et al.*, 1976) and, in addition, provides information on the total SO_2 content.

Table 8-6. SME UV ozone systematic error summary (Rusch *et al.*, 1984).

Altitude, km	Day 11	Day 101	Day 191	Day 280	rms Average
		% Error Due to Uncertainty in Sensitivity			
48	15.0	15.9	16.8	15.1	15.7
50	17.0	17.7	17.4	17.3	17.3
52	17.7	18.2	17.5	17.4	17.7
54	17.4	18.1	17.4	16.9	17.5
56	16.9	17.5	17.2	16.6	17.0
58	17.6	17.6	16.6	17.2	17.3
60	17.8	18.3	17.0	16.6	17.4
62	17.2	18.5	17.8	15.0	17.2
64	15.9	16.9	17.7	14.2	16.2
66	14.5	15.9	15.6	12.4	14.7
68	13.4	14.9	14.2	10.6	13.4
		% Error Due to Polarization Errors			
48	1.6	1.5	1.5	2.1	1.7
50	1.6	1.6	1.4	1.8	1.6
52	1.8	1.8	1.4	1.9	1.8
54	2.0	2.1	1.5	2.8	2.2
56	2.1	2.3	1.6	3.2	2.4
58	2.1	2.3	1.8	2.7	2.2
60	2.1	2.3	1.9	3.2	2.5
62	2.2	2.2	2.0	3.6	2.6
64	2.2	2.1	2.1	4.0	2.7
66	3.1	4.5	2.3	5.9	4.2
68	4.0	4.6	2.7	6.8	4.7
		% Error Due to Uncertainties in Dead Time Constants			
48	1.4	1.2	1.0	3.0	1.8
50	1.6	1.4	1.3	1.9	1.6
52	1.7	1.5	1.5	2.4	1.8
54	1.7	1.5	1.5	3.5	2.2
56	1.7	1.4	1.3	3.5	2.1
58	1.5	1.1	1.2	2.5	1.7
60	1.3	0.9	0.9	3.3	1.9
62	1.2	0.8	0.7	4.4	2.3
64	1.5	0.7	0.7	5.5	2.9
66	1.3	1.1	0.7	2.8	1.7
68	1.7	1.1	1.0	3.5	2.1
		% Error Due to Uncertainties in Ozone Absorption Cross Sections			
48	5.8	5.1	4.9	6.2	5.5
50	5.4	4.9	4.9	5.7	5.2
52	5.1	4.9	5.0	5.6	5.2
54	5.1	5.1	5.1	5.9	5.3
56	5.2	5.4	5.2	6.3	5.5
58	5.4	5.6	5.2	6.2	5.6
60	5.6	5.6	5.2	6.4	5.7
62	6.1	5.4	5.1	6.8	5.9
64	6.6	5.0	4.9	7.3	6.0
66	4.6	4.2	4.5	5.1	4.6
68	4.1	3.5	4.2	5.1	4.3
		% Error (Year Total)			
48	16.9				
50	18.3				
52	18.7				
54	18.6				
56	18.3				
58	18.4				
60	18.7				
62	18.5				
64	17.8				
66	16.1				
68	15.0				

Vertical Distribution of Ozone

8.1.1.4 Umkehr Method

Estimates of the vertical ozone distribution have been made with the Dobson instrument using the "Umkehr" effect (Gotz *et al.*, 1934).

Table 8-7. SME UV ozone random error summary (Rusch *et al.*, 1984).

Altitude, km	Day 11	Day 101	Day 191	Day 280	rms Average
		% Error Due to Noise and Data Compression			
48	2.5	3.4	2.9	4.3	3.4
50	1.9	2.5	2.2	4.1	2.8
52	2.3	2.0	2.8	4.5	3.0
54	3.3	2.4	3.8	5.4	3.9
56	3.5	3.1	4.7	5.3	4.2
58	3.1	3.6	4.9	5.2	4.3
60	4.6	4.0	4.4	7.2	5.2
62	6.3	4.9	4.9	7.3	5.9
64	6.2	6.5	7.8	8.7	7.3
66	9.5	6.6	9.6	9.4	8.8
68	11.0	7.3	11.6	10.5	10.2
		% Error Due to Temperature and Pressure Errors and Altitude Assignment of the Data			
48	3.7	4.4	4.6	5.2	4.5
50	5.4	6.8	6.7	6.9	6.5
52	6.7	8.5	8.0	8.8	8.0
54	7.5	9.4	8.6	10.5	9.1
56	7.8	9.7	8.6	10.7	9.3
58	7.4	9.4	8.3	10.0	8.8
60	6.9	8.9	7.8	10.6	8.7
62	7.2	8.4	7.5	11.0	8.6
64	7.5	8.4	7.9	12.3	9.2
66	6.1	8.6	8.9	9.4	8.4
68	7.4	10.0	11.4	11.0	10.1
		% Error (Year Total)			
48	5.6				
50	7.1				
52	8.5				
54	9.9				
56	10.3				
58	9.9				
60	10.1				
62	10.6				
64	11.9				
66	12.2				
68	14.4				

Recently, a new method for obtaining ozone profiles, known as the "short Umkehr," has been tested and accepted. The short Umkehr method requires zenith sky measurements on the A, C, and D wavelength pairs of the Dobson ozone spectrophotometer while the solar zenith angle is between 80 and 89 degrees. It has been shown by DeLuisi (1970) in a theoretical-numerical study that such measurements should contain at least as much information about the ozone profile as do the conventional Umkehr observations taken on the C wavelength pair while the solar zenith angle is between 60 and 90 degrees. The short Umkehr requires about one-third of the observing time needed for the conventional Umkehr.

This reduced observing time gives the short Umkehr at least three distinct advantages over the conventional Umkehr. First, there is less chance that significant changes in the ozone profile will occur during the course of the observation; second, there is a better chance that the zenith sky will remain clear; and third; it costs less per Umkehr observation in terms of observer time.

Hudson and Reed (1979) present the error estimates of the Umkehr method. As for the Dobson total ozone, this does not consider the impact of the Bass and Paur ozone absorption coefficients. We note that one recent development in the Umkehr measurement program has been the distribution of automated Dobson instruments at 7 sites. Instruments are currently operative at Boulder, Colorado; Mauna Loa, Hawaii; Haute Provence, France; Poker Flat, Alaska and Perth, Australia. Initiation of operations at Huancayo, Peru is planned for this year and a seventh site is under consideration.

8.1.1.5 Balloonsondes

For determinations of the vertical ozone distribution with good vertical resolution, direct soundings are required. Optical balloonsondes, using differential absorption techniques analogous to the Dobson method, were designed by Kulcke and Paetzold (1957), Vassy (1958), and Kobayashi *et al.* (1966). Above the ozone maximum, these methods have limited vertical resolution, but potentially good absolute accuracy.

Electrochemicalsondes, using the reaction of ozone with an aqueous solution of potassium iodide, were later developed by Brewer and Milford (1966), Komhyr (1965), and Kobayashi and Toyama (1966). These can be flown day or night and have better vertical resolution than the opticalsondes below 25 km. In practice, data from the electrochemicalsondes must be adjusted by coincident independent total ozone observations, and all such sondes require air pump efficiency corrections. Intercomparison between balloonsondes shows agreement within about 6 percent after corrections are applied.

The sensors in both the ECC and Brewer-Mast sondes are based on the reaction of ozone with the iodide ion to form molecular iodine, but the sondes differ in the design of the electrochemical cell. The reaction is not specific for ozone. Sulfur dioxide causes a negative interference of one mole of O_3 per mole of SO_2, while NO_2 gives a slight positive interference (Katz, 1977; Schenkel and Broder, 1982). Contamination by NO_2 should be unimportant at rural sites, where concentrations of NO_x are 0.2-10 ppbv (Logan, 1983). Surface concentrations of SO_2 at rural sites in the eastern U.S. are between 5 ppbv and 15 ppbv in winter, but below 5 ppbv during other seasons (Mueller and Hidy, 1983). Similar values are reported for southern Germany (Reiter and Kanter, 1982). Concentrations above the boundary layer are generally below 1 ppbv (Blumenthal *et al.*, 1981; Georgii and Meixner, 1980). Sonde data from the boundary layer in polluted areas may therefore be contaminated by SO_2.

Comparison of the integrated ozone profile recorded by the BM sonde with concurrent measurement of the ozone column recorded by a Dobson spectrophotometer indicates that the sonde results are too low by 10%-30% (e.g. Dütsch, 1966). Results from ECC sondes agree more closely with Dobson measurements

(Kohmyr, 1969; Torres and Bandy, 1978). In practice, individual soundings are multiplied by a correction factor, to ensure that the integrated ozone column is equal to the Dobson measurement of the ozone column. This procedure requires an estimate of the amount of ozone above the altitude reached by the sonde, about 30 km (Dütsch *et al.*, 1970). There is no real justification for this scaling procedure, since it has not been demonstrated that the response of the sondes is linear with respect to ozone over the entire altitude range. The scaling procedure introduces errors due to uncertainty in the ozone amount above 30 km and errors associated with the Dobson technique.

Intercomparison flights have shown that the ECC sonde gives higher concentrations of tropospheric ozone than the BM sonde by 12-20%, after correction to the Dobson column. Systematic differences were not apparent in the stratosphere (Attmannspacher and Dütsch, 1970; 1981). Laboratory tests in a flight simulator suggest that the ECC sonde overestimates the concentration of tropospheric ozone by 10%-15% (Barnes *et al.*, 1985). No such test results have been published for the BM sonde. De Muer (1976) reported that descent data for the BM sonde tend to be about 25% higher than ascent data in the troposphere, implying that published data (based on ascent values) may underestimate tropospheric ozone. These last results appear inconsistent with the combined conclusions of Barnes *et al.* (1985) and Attmannspacher and Dütsch (1981). Uncertainties in the response of these sondes to ozone at concentrations characteristic of the troposphere should be resolved by careful laboratory and field studies.

Although the United States funded balloon ozonesonde networks from 1964 through 1966, these measurements have been discontinued. The only station flying sondes routinely in the United States as described above is Wallops Island, Virginia, on about a weekly basis. Other than this station, our information on the vertical ozone distribution in the lower stratosphere comes from approximately 10 stations in Canada, Japan, Europe, and Australia. Error estimates of the current operational balloonsonde systems are presented by Hudson and Reed (1979).

Recently, it has been indicated that a modified electrochemical balloonsonde would be capable of reliable ozone measurements up to about 40 km. This instrument is currently being deployed at three sites; Hilo, Hawaii; Boulder, Colorado and Edmonton, Canada with once-per-week launches scheduled.

During 1983-84, a balloon ozone intercomparison campaign was conducted under NASA sponsorship whose purpose was to assess the accuracy and precision of various ozone measurement systems under development as well as those flown operationally. The results have been reported by Hilsenrath *et al.* (1984) and the following are some initial results:

The difference among 5 *in situ* UV photometers flown together was about $\pm 3\%$ during ascent to about 41 km. During float at 42 km the difference nearly doubled. During descent, the difference decreased to about $\pm 2\%$ which is much closer to the expected accuracy of these instruments. A complement of electrochemical sondes flown with the UV photometers agreed with them in the range of 0-20% depending on the sonde and altitude. Some electrochemical sondes gave systematically lower ozone values at pressures lower than 10 mbar (31 km). One comparison between an *in situ* UV and a solar absorption photometer indicated 10% difference in the stratosphere where the *in situ* measurement was lower. Balloonsondes also showed systematically lower values than concurrent Umkehr and SBUV satellite observations in this altitude range. Intercomparisons among all the instruments in the troposphere showed 20-30% differences. A comparison of pressure measurements performed by several experimenters resulted in differences as high as $\pm 15\%$ from the average measurement.

8.1.1.6 Rocketsondes

For altitudes above 30 km, optical and chemiluminescence techniques have been adapted for the sounding rocket. These methods can operate at altitudes up to approximately 70 km. The earliest successful rocket data were acquired by Johnson *et al.* (1952) using a spectrograph launched at sunrise. This technique has been more recently employed by Krueger (1969), Nagata *et al.* (1971), and Weeks and Smith (1968), using UV filter radiometers. Carver *et al.* (1966) have used the moon for nighttime measurements. Hilsenrath *et al.* (1969) have used the chemiluminescent method for day and night soundings. By use of preflight multipoint calibrations and inflight flow-rate measurements, they find agreement within 10 percent of optical results. Randhawa (1967) has used a similar method on small rockets; however, his measured ozone concentrations above 35 km are generally two to five times greater than those of the other investigators.

In September 1979, International Rocket Ozonesonde Intercomparisons were held under FAA, NASA and WMO sponsorship at Wallops Island, Virginia. Results of this intercomparison should be available in the near future.

The United States is currently operating one rocket ozone station at Wallops Island, Virginia, using a modified Krueger optical technique (Holland, personal communication). This effort is, basically, in support of satellite observations and is limited to only a few observations per year.

8.1.1.7 Lidar

The recent development of powerful tunable lasers has opened a new experimental field for spectroscopic studies of atmospheric trace constituents. As part of it, the differential absorption laser technique (DIAL) has already been used for ground-based measurements of minor constituents in the boundary layer (Cahen *et al.*, 1981, Frederiksson *et al.*, 1979; Murray *et al.*, 1977).

Vertical concentration profiles of atmospheric ozone have also been recorded by using UV and IR lidar systems; however, these measurements have been restricted either to the boundary layer (e.g., Asai *et al.*, 1979; Bufton *et al.*, 1979: Browell *et al*, 1981) or to the stratosphere (Megie *et al.*, 1977; Uchino *et al.*, 1980). Pelon and Megie (1982a) describe the evaluation and realization of a ground-based UV lidar system for continuous monitoring of the ozone number density profile from the ground up to the 25-30 km range.

The emission performances of the laser system and the receiver characteristics have been summarized by Pelon and Megie (1982a). The full sequence of a DIAL measurement is computer controlled and a real time analysis of the data can be performed. The reliability of the various subsystems and experimental procedures have been tested during several field experiments in 1980-1981. The main characteristics of the measurements can be summarized as follows:

— Vertical profiles of the ozone number density are obtained for clear sky conditions from the ground up to 25 km. This altitude range has been recently extended up to 40 km (Pelon and Megie, 1982b).

Three ozone profiles corresponding to the altitude ranges 0-8 km, 7-17 km, 15-28 km are successively obtained within a 15 min acquisition time. This sequential experimental procedure results from the optimization criteria of the DIAL method.

The relative accuracy corresponding to a 1σ standard deviation on the ozone number density for each individual profile is:

(1) Better than 5% at tropospheric altitude levels for a vertical resolution of 450 m.

(2) Minimum in the 23-28 km altitude range where it decreases down to 20% at the uppermost level for a vertical resolution of 1.2 km and a 15 min. acquisition time.

8.1.2. Satellite Data Comparisons

As described above, a critical element of this chapter is a discussion of the comparison of SBUV versus other types of data to provide evidence of the absolute accuracy of the profile. Within the previous section we have discussed the comparisons with ground-based information; in this section we will focus on the satellite intercomparisons. Specifically, in April 1979 the SBUV, LIMS and SAGE instruments were all operative and as they utilize three entirely different measurement techniques their comparisons provide an excellent opportunity to assess our capability to measure ozone in an absolute sense.

Inasmuch as actual overpass coincidences of the satellite data are very few, our approach is to compare the zonal average for the month, recognizing that the SAGE coverage is inherently more limited than the others at a specific latitude. For these comparisons the SBUV Ozone Processing Team has recalculated the zonal averages utilizing the algorithm with the updated absorption coefficients (Bhartia and Fleig, personal communication) such that the latest estimates of each data set are provided.

The results for 45 °N (actually 44 °N for LIMS and SBUV) and the Equator are presented in Figure 8-3. At 45 °N we see that there is, overall, very good agreement in the shape of the 3 profiles with the largest disparity in the lower stratosphere between about 30 to 10 mbar. Standard deviations of the three data sets are included both in ppmv and percentage of the mean at 30–, 10–, 5–, 2–, 1 and 0.5 mbar. We see that in the middle stratosphere the agreement is excellent and the standard deviation is only about 3%. Above this level the standard deviation increases to about 7% and in the lower levels increases to about 15%.

At the Equator we see that SAGE and SBUV are in agreement at the lower levels with LIMS larger than either, but that SAGE then crosses over to indicate the largest maximum of the three data sets. Above the maximum SBUV and LIMS show very good agreement with SAGE considerably greater than the others. The relative maximum in the SAGE data at about 1.5 mbar results in an increase of the standard deviation at 2 mbar to about 10% versus its value of about 3% at 45 °N.

On the basis of the above, one can see that it is very difficult with such a limited sample to ascribe specific limits of uncertainty in the absolute value of the measured ozone. Therefore, for discussion purposes later in this section we suggest the following (1 standard deviation) limits as representing our capability to determine ozone in an absolute sense from satellite data:

- 15% 30 to 10 mbar
- 6% 10 to 0.5 mbar

Note that the above estimates are well within the RMS of the instrument systematic error summaries above of about 30% and 16%, respectively.

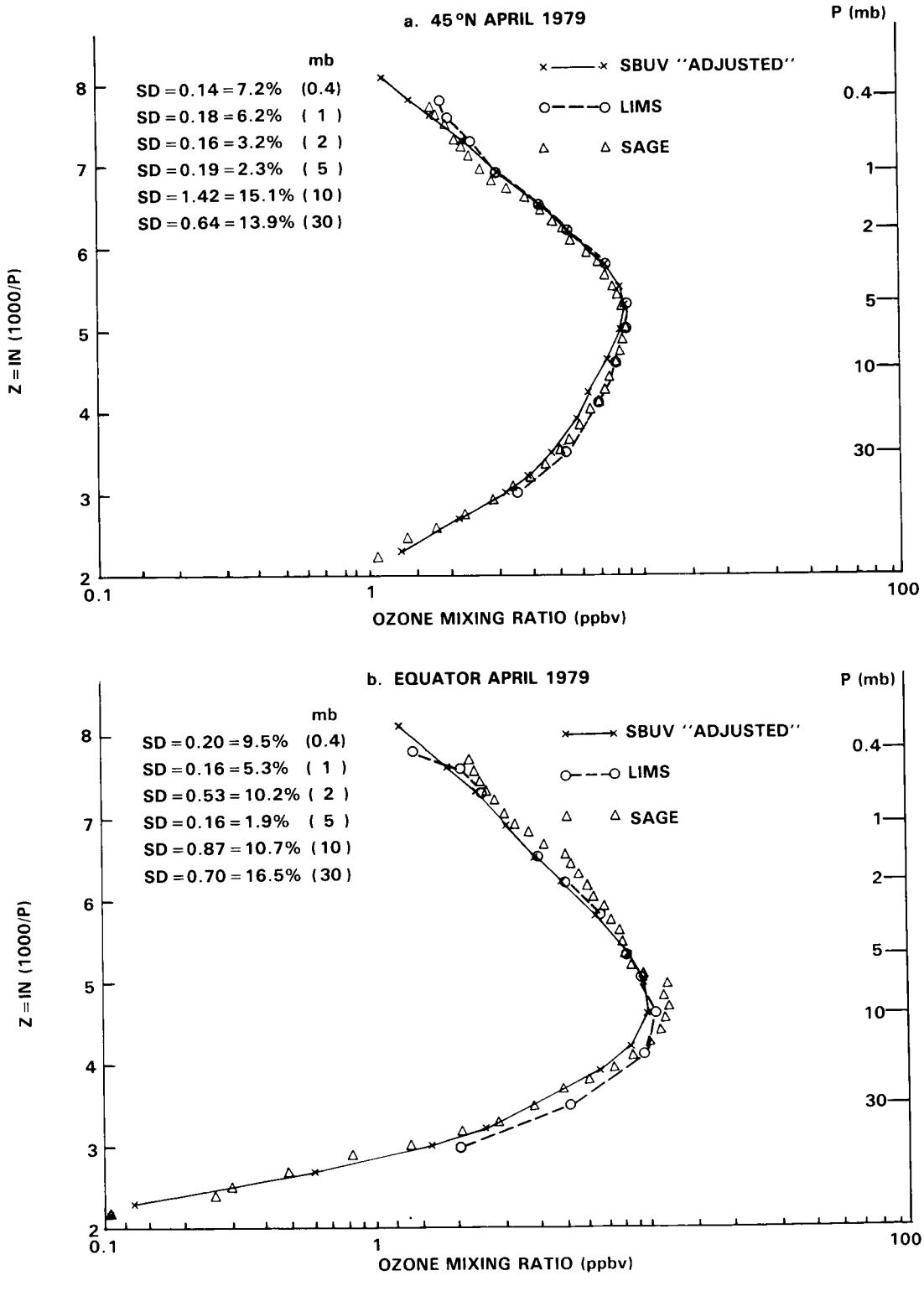

Figure 8-3. Monthly average ozone profile (ppmv) for April 1979 SBUV, LIMS and SAGE instruments at 45°N (a) and Equator (b).

8.1.3 Confidence Estimation of Mean Monthly Zonal Averages

When we compute a mean monthly zonal average ozone profile, there are several sources of error as well as natural variability that must be considered. Specified in terms of standard deviation, these are:

S_1 — the random measurement errors of the SBUV instrument;

S_2 — the random error of the daily true zonal average due to incomplete sampling (i.e., 14 points per day) extended to the domain of a monthly average;

S_3 — natural variability within a month, i.e., representativeness of the monthly average;

S_4 — natural year-to-year variability, representativeness of the multiyear average;

S_5 — absolute value of the measurement system.

The first two components have been extensively covered in the National Plan for Stratospheric Ozone Monitoring (FCM, 1982) and will be briefly summarized here.

For the SBUV instrument, the random error term, S_1, is estimated to be about 2.5% for total ozone and about 10% for the vertical distribution. When we determine the zonal average over a 5° latitude band, this encompasses about 28 data points. The contribution to the total uncertainty variance is:

$$\text{a)}\ \frac{S_1^2}{28 \times 30} = \frac{(25)^2}{840} = 0.007\%\ \text{total}$$

$$\text{b)}\ \frac{S_1^2}{28 \times 30} = \frac{(10)^2}{840} = 0.12\%\ \text{vertical profile}$$

When we determine the 5° daily zonal average from the 28 data points, however, an additional sampling error occurs due to incomplete sampling of the traveling wave patterns. This is about 1% for the SBUV (Wilcox, personal communication). We will assume this to be independent of pressure, although this is most likely very conservative for the profiles. Also, we will assume that the sampling errors are correlated in time such that there are only 10 independent observations per month. The contribution of this term to the uncertainty variance is:

$$\frac{S_2^2}{10} = \frac{(1)^2}{10} = 0.10\%$$

In the case of the S_3 component, which is the representativeness of the monthly average value or the error in utilizing the daily measured values to determine the monthly average, we have made the assumption that there are only 10 independent data points during the month. The results are indicated in Table 8-8 for the 4 months of depiction at low-, mid- and high-latitudes for 30- and 1- mbar. We see that the within month standard error is generally within 2%, but that it can be as large as 7% during certain periods such as high-latitude winter.

Table 8-8. SBUV Within Month Standard Error (%) 1978–1979.

	30 mbar	1 mbar
January		
70	7	7
40	4	3
0	2	2
−40	2	2
−80	2	1
April		
80	3	3
40	2	1
0	1	1
−40	2	2
−80	4	1
July		
80	1	2
40	1	2
0	2	1
−40	2	6
−70	1	4
October		
80	4	1
40	2	2
0	2	1
−40	2	3
−70	7	3

For the profile comparisons, then, we should utilize the following values of S_3^2

$S_3^2 = 4$ low-latitude and summer

$S_3^2 = 16$ mid- and high-latitude spring/fall

$S_3^2 = 49$ mid- and high-latitude winter

A subtle point is raised in this regard in that with the virtually complete sample of SBUV (at least in daytime) the variation within month does not represent an error or uncertainty in the monthly average. As the current models seek to emulate only the monthly average and not a daily value, inclusion of this term in the overall uncertainty is not warranted at this time. At such time when three-dimensional models are available this term should be included within the comparisons.

For the S_4 term that encompasses the natural variability we have little or no indication from theory as to what to expect save possibly that due to solar variations. We, however, consider that to be a "regular" feature that we should be able to detect and not part of the year-to-year variability. With no theoretical framework to guide us, we have utilized the 4 year SBUV record and calculated at 10° latitude increments the standard deviation between years for the 4 year average. The results at 60°N, equator and 60°S are presented in Figure 8-4 as a function of pressure and month. The standard error is the standard deviation divided by 2.

We see that the standard deviation calculated in this manner, which includes certain elements of S_3, is relatively small being generally on the order of 4% or less. The exception is the winter of each hemisphere where it becomes about 6% at 1 mbar of the Northern Hemisphere and 8% for the Southern Hemisphere. On this basis we will utilize values of S_4^2 (standard error) as follows:

S_4^2 = 4 low-latitude, summer and spring

S_4^2 = 16 mid-and high-latitude winter

Adding the measurement variances plus the year-to-year variance, while excluding the within month variance as described above, we see that the uncertainty of the monthly average is dominated by the year-to-year variation. For purposes of estimating the uncertainties of the SBUV profiles, then, we will utilize the following values:

σ (%) = 2% Low-latitude, summer, spring, fall

σ (%) = 4% Mid-and high latitudes winter

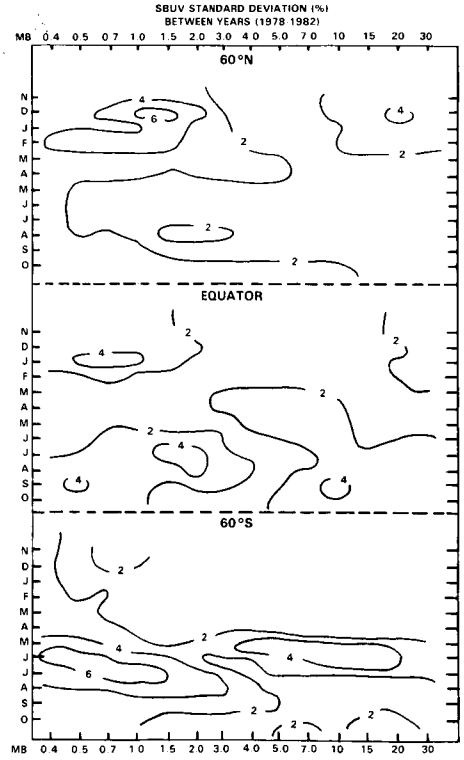

Figure 8-4. SBUV standard deviation (percent) between years (1978–1981) at 60°N (top), Equator (middle) and 60°S (bottom).

8.1.4 Average Vertical Profiles/Total Ozone

In the last section we combine the various elements described above to present our "best" estimate of the vertical ozone profiles/total ozone values along with the uncertainty estimates as determined from the previous elements. Presented in Figures 8-5 and 8-6 are the vertical ozone profiles (in units of volume mixing ratio ppmv) as a function of height with the following scales:

- The vertical scale is linear with scale height, defined as $Z = \ln(1000/P)$
- Included also are the decadal units of pressure in mbar along with the geometric altitude (km) as determined by multiplying Z by the approximate scale height of 7 km (Standard Atmosphere, 1966). Note that over an annual cycle the geometric altitude may change by several kilometers so that these values should be regarded as approximate only.

In order to provide information over the annual cycle and latitude domain we have selected for presentation the following data:

- Months: January, July
- Latitude: Equator, 30°N, 30°S, 45°N, 45°S, 60°N, 60°S

For each data source the curves are based on:

- Balloonsondes — The data are averaged for the period 1979-1983 in Umkehr layers within the latitude bands, 52.5-90°N(60°N), 37.5-52.5°N(45°N), 15°S-15°N(Equator), 37.5-52.5°S(45°S) and 52.5-90°S(60°S) (Hilsenrath, private communication).
- SBUV — The data are averaged for the period Nov. 1978 — Oct. 1981 at the specific latitudes as interpolated from the monthly average synoptic charts. This includes the total ozone value.
- Adjusted SBUV — These are the SBUV profiles multiplied by an average adjustment factor provided by the SBUV Ozone Processing Team (private communication) mainly to account for the recently adopted ozone absorption coefficients. Such adjustments are presented to indicate the sign and magnitude of their effect as is anticipated for the final processed data.
- SME (UV and IR) — The data are averaged for the period 1982-1984. Note that as described above the longitudinal coverage is not complete.

As a simple consistency check we have calculated the total ozone from the SBUV profiles from 0.4 to 30 mbar and the balloonsondes from 30 to 1000 mbar and compared the results against the SBUV total ozone measurements. The results are presented in Table 8-9. From above we would anticipate that the SBUV total ozone should be on the order of 8% lower than the combined SBUV-balloonsonde calculations. This is because the balloonsondes are normalized to the Dobson measurements and the SBUV is about 8% lower than the Dobsons. If the combined total ozone is very different from the 8% value then this raises the question of representativeness of the balloon profile possibly due to the number of stations in the region and/or to the number of points at the stations.

Table 8-9. Comparison of Total Ozone Calculated from Ozone Profile Versus Total Ozone Determined from SBUV.

60°N	Jan.	April	July	Oct.
SBUV (.4-30 mb)	117.1	133.9	129.5	121.5
Balloonsondes (30-1000 mb)	283.9	329.4	236.0	212.4
Total	401.0	463.3	365.5	333.9
SBUV	362.0	399.7	319.3	291.8
SBUV — Total (%)	−9.7%	−14.2%	−12.6%	−12.6%

45°N	Jan.	April	July	Oct.
SBUV (.4-30 mb)	134.0	148.5	150.3	140.3
Balloonsondes (30-1000 mb)	220.6	258.9	193.5	165.2
Total	354.6	407.4	343.8	305.5
SBUV	340.7	360.4	307.1	277.5
SBUV — Total (%)	−3.9%	−11.5%	−10.7%	−9.2%

30°N	Jan.	April	July	Oct.
SBUV (.4-30 mb)	145.2	161.9	165.1	158.8
Balloonsondes (30-1000 mb)	182.4	211.2	—	117.8
Total	327.6	373.1	—	276.6
SBUV	269.9	300.5	279.7	258.2
SBUV — Total (%)	−17.6%	−19.5%	—	−6.7%

Equator	Jan.	April	July	Oct.
SBUV (.4-30 mb)	174.3	176.3	176.1	178.1
Balloonsondes (30-1000 mb)	82.6	84.3	97.0	129.0
Total	256.9	260.6	273.1	307.1
SBUV	230.9	239.3	245.7	245.2
SBUV — Total (%)	−10.1%	−8.2%	−10.0%	−20.2%

45°S	Jan.	April	July	Oct.
SBUV (.4-30 mb)	150.2	139.1	129.4	148.0
Balloonsondes (30-1000 mb)	124.6	152.2	206.6	190.7
Total	274.8	291.3	336.0	338.7
SBUV	292.6	273.5	308.9	338.0
SBUV — Total (%)	+6.5%	−6.1%	−8.1%	−0.2%

From Table 8-9 we see that the latitudes with the best consistency are 45 °N, where the largest number of stations exist, and the equator, where the fewer observations seem to have lesser impact. The significant exception to this is in October at the Equator where the balloonsondes indicate very large values that do not appear reasonable. At the other latitudes the results appear to be more sensitive to the available data and the comparisons in the region should be made with appropriate care.

For the upper level profiles, looking first at January — Equator, Figure 8-5 (d) we see overall excellent agreement of the SME-IR data with the SBUV data in the overlap region. The SME-UV data indicate a positive bias against the others although the two SME curves tend to merge at about 1 mbar. SBUV adjusted values tend to be lower than unadjusted values with the major impact in the lower layers.

As we move away from the Equator into the Northern Hemisphere we see increasing disparity of SME, both with SBUV and with itself. The former is undoubtedly due in part to the limited sampling in the winter hemisphere while the latter must be due to the instrument/algorithm differences. In the Southern, summer Hemisphere the overall agreement is much better, but SME maintains a positive bias. Note also that toward higher latitudes the sense of the SBUV adjustment changes at the lower levels with the adjusted SBUV larger than unadjusted.

For the Southern Hemisphere winter, July, Figure 8-6, we see that a similar pattern emerges with the SME greater than SBUV with the tendency of the two to merge at about the 1 mbar level. The summer SME values are quite consistent as was the case for Southern Hemisphere January profiles, but we note that the winter values seem more consistent than their Northern Hemisphere counterparts.

Finally, in the previous sections we have attempted to resolve the question as to the uncertainties in the average profiles and have divided the uncertainities into absolute and random components. In this section we combine the two components to achieve what we feel is our best estimate of the overall uncertainties and in Figures 8-5 and 8-6 we plot the two standard deviation uncertainty bars at 1 and 10 mbar. The values are based on the following combined elements:

- Low latitude/summer/spring/fall

  30-10 mbar $1\sigma = 15.1\%$ $2\sigma = 30.2\%$

  10-0.4 mbar $1\sigma = 6.3\%$ $2\sigma = 12.6\%$

- Mid- and high-latitude winter

  30-10 mbar $1\sigma = 15.5\%$ $2\sigma = 31.0\%$

  10-0.4 mbar $1\sigma = 7.2\%$ $2\sigma = 14.4\%$

8.2 COMPARISON OF CALCULATED AND OBSERVED OZONE PROFILES

Total ozone has been observed for many years at various stations located in different parts of the world. A climatology of these data has been presented for example by London (1980b), indicating that the average ozone column reaches a maximum between 70 and 75 °N at the end of March and that the maximum observed in the Southern hemisphere is smaller and located at somewhat lower latitudes and earlier in the season, than that of the Northern Hemisphere. Two-dimensional time-dependent models with a classical Eulerian or a diabatic circulation can produce satisfactory fits to the above observations. Moreover, as shown by Figure 8-7a and b, the meridional distribution of ozone provided by 2-D models below 35 km

ORIGINAL PAGE
COLOR PHOTOGRAPH

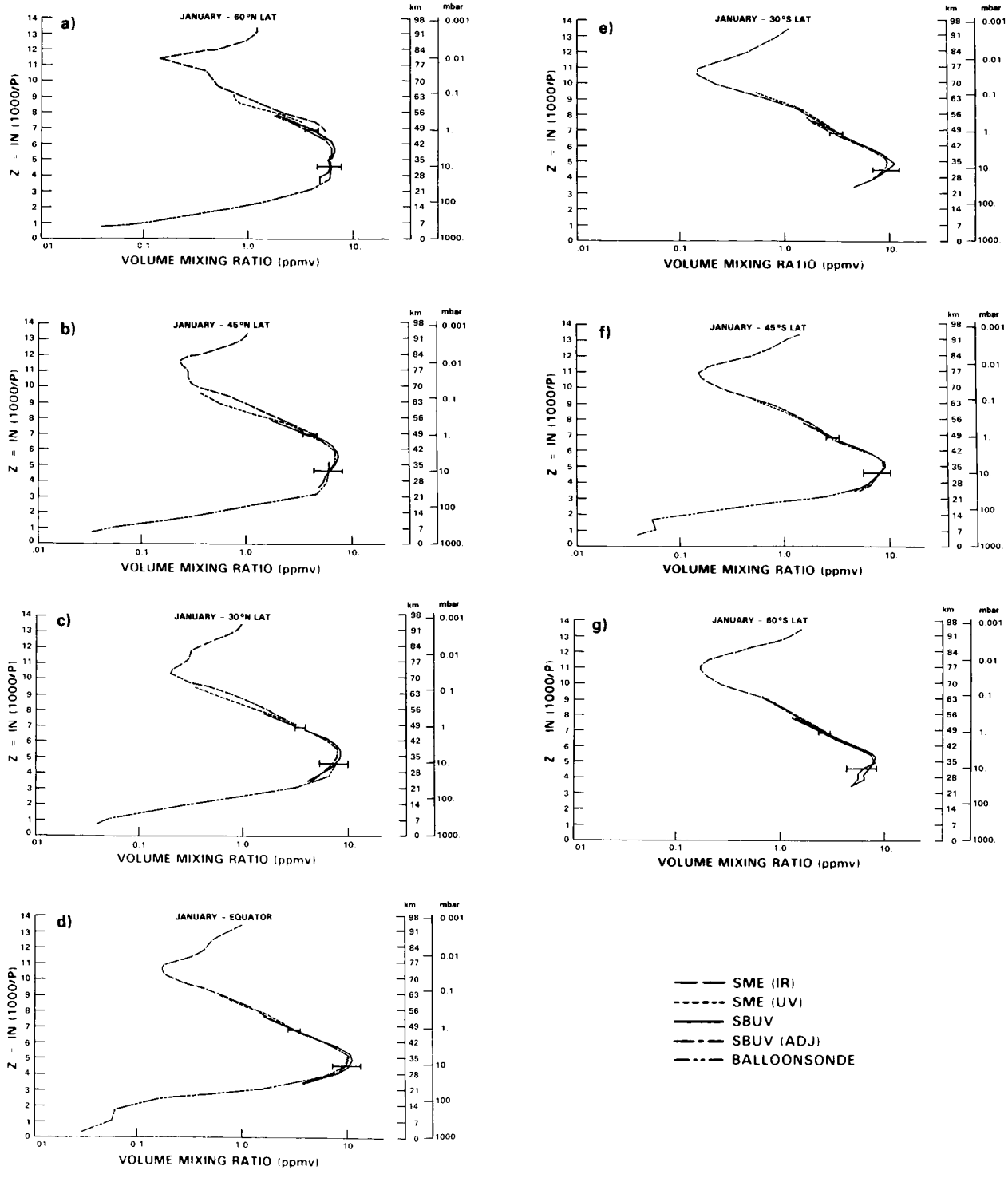

Figure 8-5. Average ozone vertical profiles (ppmv) for January at 60°N (a), 45°N (b), 30°N (c), Equator (d), 30°S (e), 45°S (f) and 60°S (g) for SME (UV and IR), SBUV (adjusted for Bass and Paur coefficients and unadjusted) and balloonsondes. Also plotted are 95% uncertainty bars (see text) on SBUV data at 1- and 10-mbar.

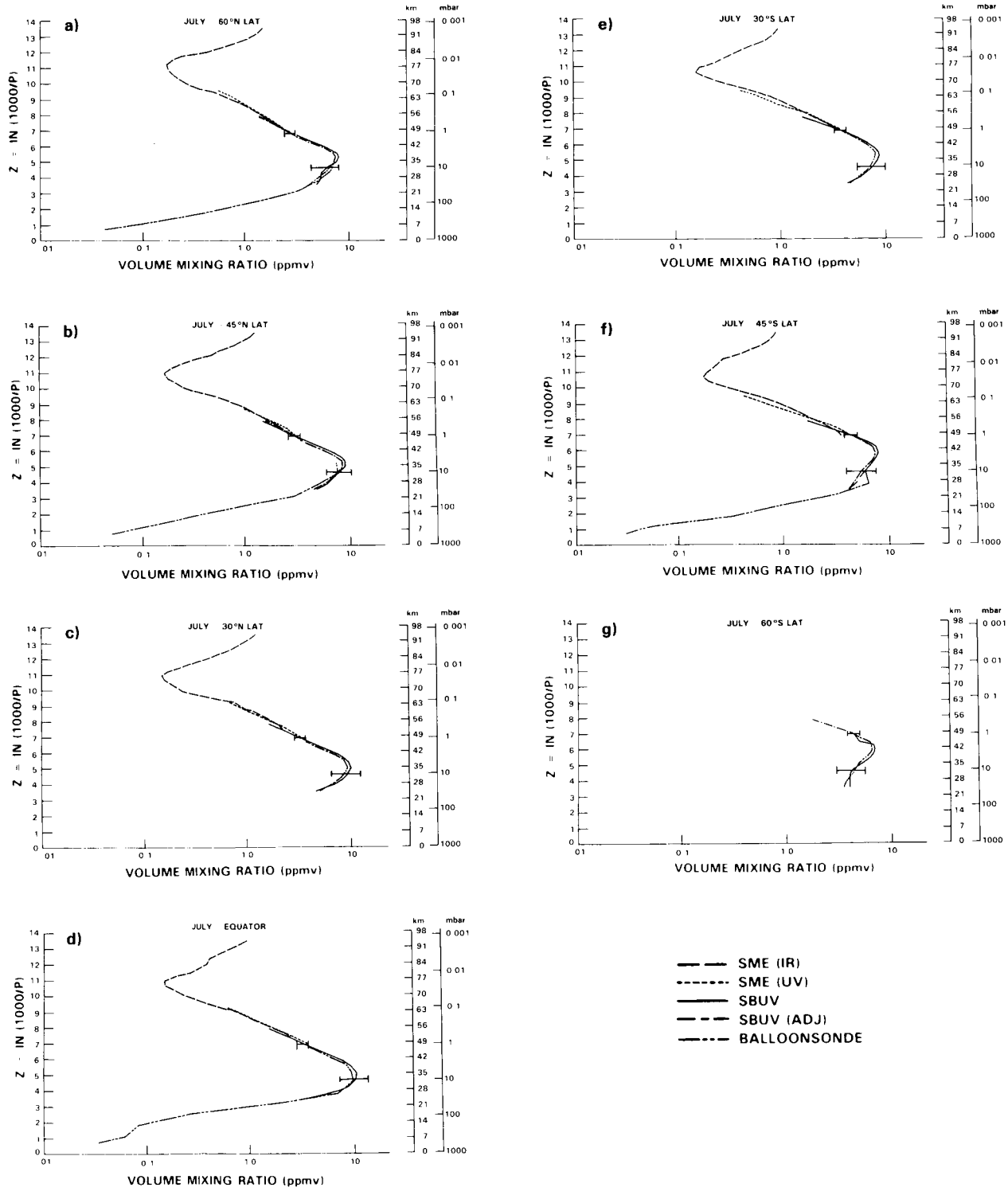

Figure 8-6. Average ozone vertical profiles (ppmv) for July at 60°N (a), 45°N (b), 30°N (c), Equator (d), 30°S (e), 45°S (f) and 60°S (g) for SME (UV and IR), SBUV (adjusted for Bass and Paur coefficients and unadjusted) and baloonsondes. Also plotted are 95% uncertainty bars (see text) on SBUV data at 1- and 10-mbar.

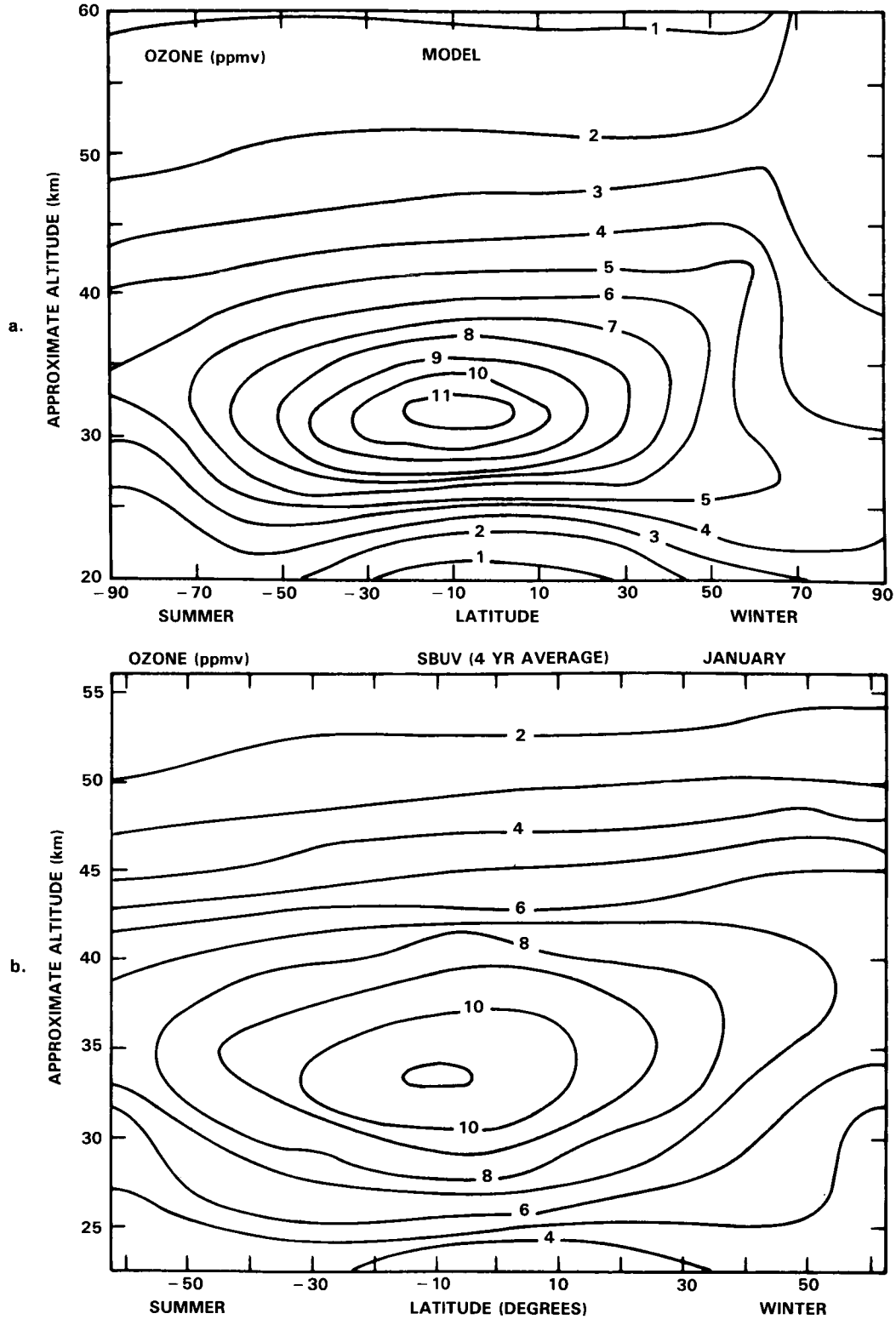

Figure 8-7. Two dimensional distribution of the ozone mixing ratio (ppmv).
(a) : Model calculation by Solomon et al. (1985b).
(b) : Four year average of SBUV data.

are in good agreement with the climatology of O_3 resulting from satellite observations. These results, however, depend more on the transport parameterization than on the chemical scheme adopted in the model. A validation of the chemistry should preferably deal with comparisons of ozone distributions in the upper stratosphere and in the mesosphere.

In addition to numerous rocket and balloon observations, space borne experiments (SBUV, LIMS, SAGE, SME and ATMOS) have provided a large data base of ozone concentrations in the region where photochemical equilibrium conditions should apply to O_3. The standard deviation arising from comparisons between a subset of these observations (see previous sections) using completely different techniques, is about 6 percent above 6 mbar whereas there are significantly larger systematic uncertainties in each experiment, so that the reported vertical profiles can essentially be considered to represent absolute values.

Several model calculations in the stratosphere (Ko and Sze, 1983; Froidevaux *et al.*, 1985a; as well as those reported in Chapter 12) and in the mesosphere (Prather, 1981; Solomon *et al.*, 1983; Allen *et al.*, 1984; Aikin *et al.*, 1984; Rusch and Eckman, 1985) have been used for an interpretation of ozone data. The more recent studies generally include a reduced O_2 absorption cross section in the Herzberg continuum, as suggested by the stratospheric solar flux measurements of Frederick and Mentall (1982), Hermann and Mentall (1982), Anderson and Hall (1983), as well as the laboratory work of Cheung *et al.* (1984) and Johnston *et al.* (1984). Note however that the cross sections derived by Pirre *et al.* (1985) from flux measuremenis in the stratosphere are higher than the data deduced from the other recent experiments. As indicated by Froidevaux and Yung (1982), Brasseur *et al.* (1983b), Ko and Sze (1983) and Jackman and Guthrie (1985), the use of these lower O_2 cross sections (see Chapter 7) has reduced the calculated concentrations of several gases, in particular ozone, in the middle and upper stratosphere.

Figure 8-8 shows the range of ozone mixing ratios calculated at 30°N for winter and summer conditions by the two-dimensional models under consideration in this report. The profile from the Rutherford Appleton Laboratory, however, has not been included in the figure since this model uses a very low chlorine abundance. The model range is typically $\pm 20\%$ about the average profile, which probably reflects the combined effects of slightly different dynamical and photochemical representations, in addition to the seasonal effects. These theoretical profiles are compared with a representative distribution of the ozone mixing ratio for January and July, respectively, based on SME (UV and IR), SBUV and balloon ozonesondes (see Figure 8-5). Also shown at selected levels for historical comparison are the ozone values (and their standard deviation) of the U.S. Standard Atmosphere, 1976. Other measurements at northern mid-latitudes, such as the OGO 4 BUV satellite data (London *et al.*, 1977), the SAGE data (Reiter and McCormick, 1982) and the LIMS data (Remsberg *et al.*, 1984a), generally fall within the bounds of this Standard Atmosphere.

In the upper stratosphere, the 2-D model results appearing in Figure 8-8, as well as recent 1-D model calculations (e.g. Ko and Sze, 1983; Froidevaux, 1983; Froidevaux *et al.*, 1985a; Brasseur *et al.*, 1985) predict concentrations which are 30 to 50 percent lower than the values representative of mid-latitude observations. Similar discrepancies in the mesosphere have been found from SME data (Solomon *et al.*, 1983a; Rusch and Eckman, 1985). Since the temperature in the middle atmosphere is directly controlled by the ozone amount, the absolute temperature value derived by radiative models should be somewhat underestimated, especially near the stratopause, if the low O_3 concentration currently predicted by photochemical models is used.

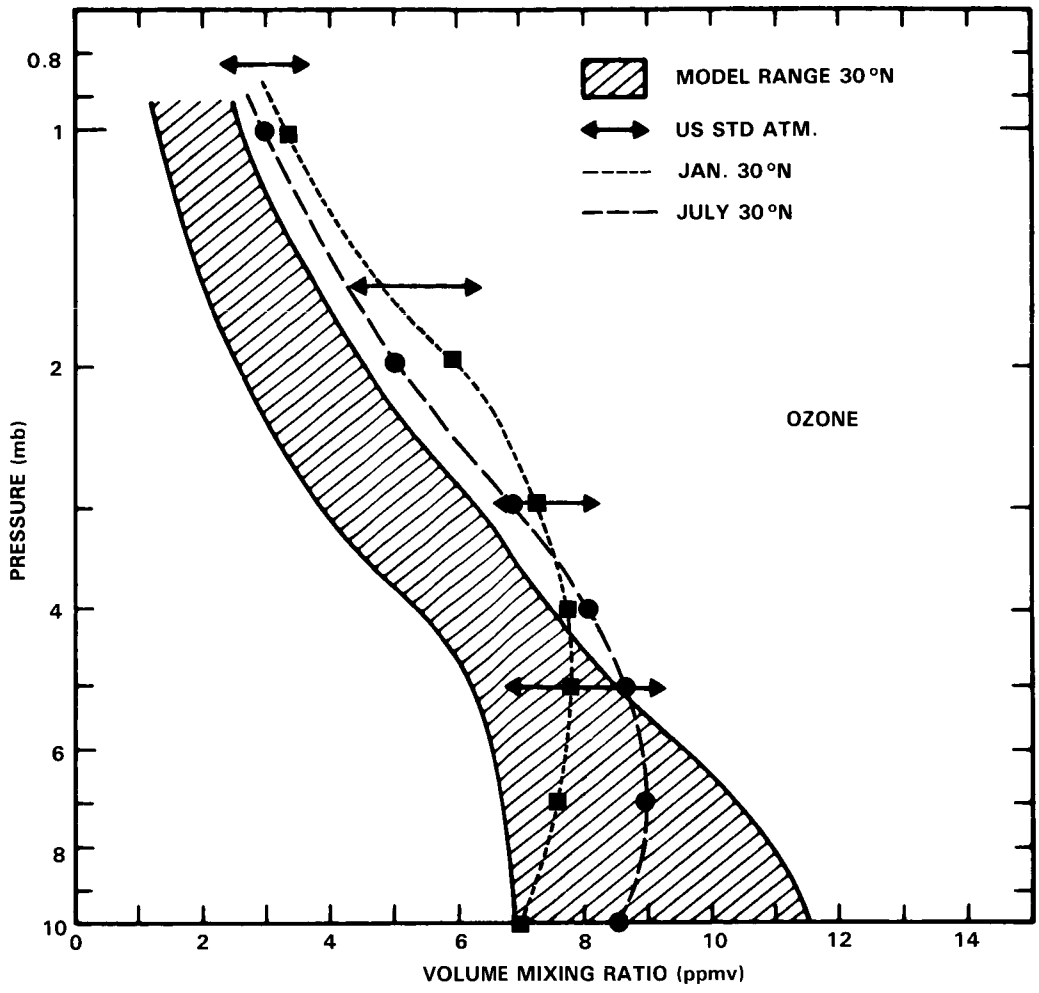

Figure 8-8. Vertical distribution of the ozone mixing ratio in the upper stratosphere. The shaded area includes 2-D model results obtained for winter and summer conditions at 30°N (see Chapter 12). The O_3 mixing ratio given by the US Standard Atmosphere as well as representative observations at 30°N for January and July are also indicated. (See Figures 8-5 and 8-6.)

In order to attempt to understand the source of these discrepancies, the uncertainties in the production and loss processes due to all catalyzing mechanisms and involving O_x, HO_x, NO_x, and ClO_x should first be investigated. In the altitude range where photochemical equilibrium conditions are satisfied, the ozone balance can be written

$$P(O_x) = L_{O_x} + L_{HO_x} + L_{NO_x} + L_{ClO_x} = L(O_x) \tag{4}$$

or, to a good approximation, (Johnston and Podolske, 1978; Froidevaux *et al.*, 1985a)

$$J_{O_2}(O_2) = k_1 (O)(O_3) + k_2 (O)(HO_2)$$

$$+ k_3 (O_3)(HO_2) + k_4 (O_3)(H) + k_5 (O)(NO_2)$$

$$+ k_6 (O)(ClO) \tag{5}$$

where the i^{th} k value represents the rate constant for the reactions between the species in the i^{th} term on the right-hand side of the above equation.

These source and sink terms in the stratosphere have been evaluated by Schmailzl and Crutzen (1985), using N_2O and CH_4 distributions from SAMS (Jones and Pyle, 1984), ozone from LIMS (Gille and Russell, 1984) or SBUV (Frederick *et al.*, 1983b), water vapor and temperature from LIMS. The distributions of other species, including ClO_x, were calculated with a 2-D model. A significant imbalance in the odd oxygen budget is found with an overproduction in the lower stratosphere and an extra loss above 30 km.

Schmailzl and Crutzen (1985) indicate that, in order to balance the ozone budget, one requires either a smaller NO production rate compared to the one derived from the SAMS N_2O data or modifications in the chemical scheme which is used for stratospheric studies.

Jackman *et al.* (1985a,b) have done a similar study using the LIMS data for O_3, H_2O, HNO_3, NO_2 and temperature in a zonally averaged form. Adopting a ClO_x mixing ratio of 3 ppbv at the stratopause and fixing CH_4 according to the SAMS data, they have calculated the $L(O_x)/ P(O_x)$ ratio for different months during which LIMS was operating. An example is given by Figure 8-9. Again, the ozone budget is unbalanced, as values of $L(O_x)/P(O_x)$ of 1.3 to 1.5 are found in the photochemical region. These results are in good agreement with those of Schmailzl and Crutzen (1985). While the imbalance is quite large, Jackman *et al.* (1986) point out that the total model uncertainty associated with the value of $L(O_x)/P(O_x)$ is close to 1.7, so that the imbalance may still be due to inaccuracies in the included chemistry and species concentrations.

Frederick *et al.* (1984) also find that the expected ozone abundances are 20-27% below the SBUV data for pressures less than 7.8 mbar, and that the observed seasonal behavior (phase) is also in some disagreement with calculations. Analyses of LIMS data also show the existence of a model ozone deficit in the upper stratosphere and lower mesosphere (Froidevaux *et al.*, 1985b).

While it is true that the error bars associated with both model and observational ozone results overlap, it is not very satisfying to interpret this as an indication that there is really no problem in modelling ozone in the upper stratosphere and lower mesosphere. Froidevaux *et al.* (1985a) have performed a sensitivity analysis (with a 1-D model) which shows that no reasonable change in any one or two parameters can resolve the systematic model ozone deficit. They argue that the (O) to (O_3) ratio is an important quantity, since the atomic oxygen concentration enters in most of the odd oxygen loss terms (Equation (5). In view of the fact that there exists only one simultaneous measurement of O and O_3 (Anderson, 1980), and that this particular determination seems to have been affected by systematic errors in the O_3 observation (see Froidevaux *et al.*, 1985a), new *in situ* determinations of the (O) to (O_3) ratio are needed in order to test the "pure O_x" chemical system in isolation.

Indeed, according to the current ozone theory, the O to O_3 concentration ratio is given by the simple expression

$$\frac{[O]}{[O_3]} = \frac{J_{O_3}}{k(T)\,[M]\,[O_2]} = \frac{J_{O_3}}{0.21\,k(T)\,[M]^2} \qquad (6)$$

where J_{O_3} is the photodissociation frequency of ozone, [M] is the total concentration and k(T) the temperature dependent rate constant of reaction $O + O_2 + M$. The pure odd oxygen chemistry can thus

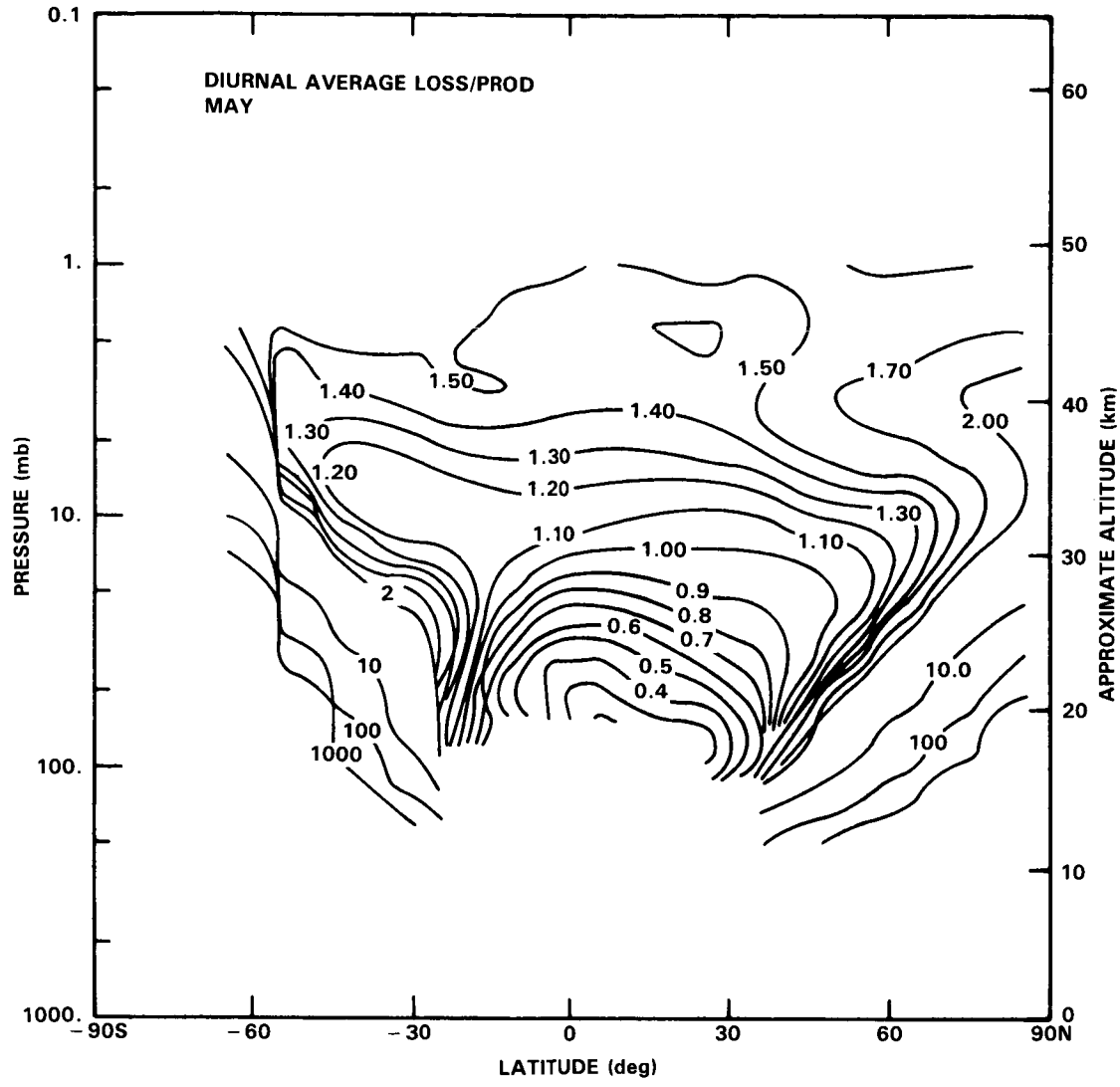

Figure 8-9. Calculated ratio of the odd oxygen loss rate to the production rate making use of temperature and trace species concentration reported by LIMS and SAMS in May 1979 (from Jackman *et al.*, 1986).

easily be tested by measuring simultaneously, at a given pressure level, the O and O_3 concentrations together with the temperature and the O_3 column density above this level. The photodissociation coefficient of O_3 can be estimated without significant error for a given solar zenith angle, assuming that the spectral distribution of the solar irradiance and of the O_3 (and O_2) absorption cross section are accurately known.

This conceptually simple chemical test has never been made so far, despite the fact that the destruction rate of odd oxygen or concentration ratios such as [NO]/[NO_2] or [Cl]/[ClO] in the upper stratosphere are usually derived by assuming that expression (6) is verified.

Finally it should be stated, as mentioned by Pallister and Tuck (1983) that a detailed observation of the 24 hour waveform of the ozone concentration in the upper stratosphere also provides a means of testing current photochemical mechanisms. For this purpose, measurements require good relative rather than good absolute accuracy. Such useful measurements have begun to be exploited by Aimedieu *et al.* (1981).

Given the ozone imbalance in the upper stratosphere and mesosphere, and the fact that dynamical effects on the mean ozone value are generally expected to be small throughout most of that region (note that 2-D and 1-D models both yield similarly low O_3 values), one is left with three main options in order to reduce or eliminate this imbalance:

1) In the currently accepted photochemical scheme, find a way to decrease the odd oxygen loss rate (whereby increasing the ozone abundance).

2) In the currently accepted photochemical scheme, find a way to increase the odd oxygen production rate.

3) Change the currently accepted photochemical scheme, so as to eliminate the ozone discrepancy.

In all the above cases, the resulting changes in species concentrations other than $[O_3]$ should not be so large as to produce significant problems of another kind. Currently, it does not appear that the mean observed concentration of HO_x, NO_x and ClO_x are systematically and significantly overestimated by the models, although there is still enough uncertainty in the observed distribution of these species not to preclude changes in their model concentrations that could reduce the ozone imbalance.

In the mesosphere, where the odd hydrogen photochemistry dominates, HO_x related sensitivity analyses need to be performed in order to try to understand differences between models and observations (see Allen *et al.*, 1984). The model ozone deficit in comparison with SME data (see Figure 8-10) could indeed be explained by errors in the hydrogen chemistry. The mesospheric water vapor abundance and

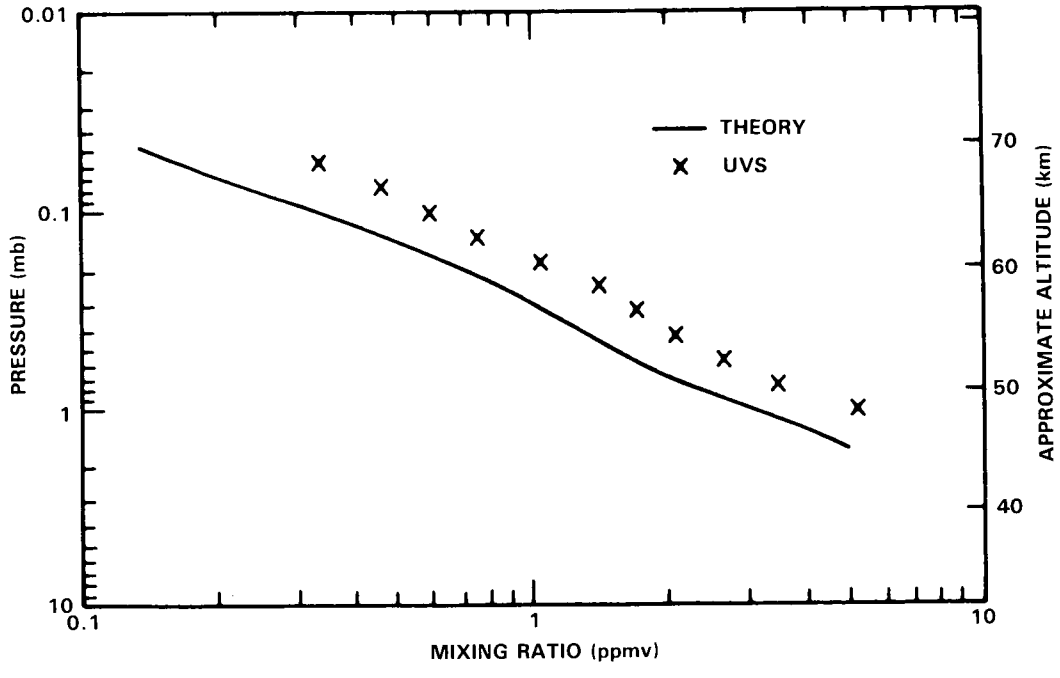

Figure 8-10. Comparison of measured weekly averaged ozone mixing ratio (crosses) to model calculations (solid line) for day 360 of 1983 (latitude 40°, solar zenith angle 76.4°). Data are from the Solar Mesosphere Explorer (from Rusch and Eckman, 1985).

some HO_x-related photochemical parameters are not very well known, nor are the rates of O_2 and H_2O photolysis in the Schumann-Runge bands (Solomon *et al.*, 1983a; Rusch and Eckman, 1985). The latter authors find that good agreement with the measurements can be obtained if the efficiency of the odd hydrogen catalytic cycle is decreased by 30-50%. One notes that even if such a change is not unreasonable (and within the total uncertainty associated with model parameters and concentrations), this type of reduction in the HO_x catalytic efficiency will have very little impact on ozone in the 35-45 km region, where a significant discrepancy also exists.

In terms of the odd oxygen production rate, there are clearly some remaining uncertainties in the photodissociation rate of O_2 in the Schumann-Runge bands and Herzberg continuum, despite recent analyses of the cross section values in those wavelength regions. A large increase in J_{O_2} (by about a factor of two) would be required in order to eliminate the ozone discrepancy above 35 km. It does not appear that such a change is within the range of uncertainty in J_{O_2} given current laboratory work. In fact, recent reductions in the measured Herzberg continuum cross sections have led to a decrease in J_{O_2} and (O_3) in the upper stratosphere. In the Schumann-Runge bands, a decrease in the underlying continuum absorption could lead to some increase in the upper stratospheric flux at those wavelengths, although the effect on JO is diluted by the Herzberg region. Nevertheless, further high-resolution laboratory studies in the Schumann-Runge bands could be worthwhile.

Possibly important additional sources of odd oxygen have been considered (this case now refers to option 3, i.e. missing chemistry). For example, Cicerone and McCrumb (1980) have indicated that the photodissociation of heavy molecular oxygen ($^{18}O\ ^{16}O$) might provide a source of odd oxygen in the atmosphere. A recent line by line calculation of the related photodissociation coefficient by Blake *et al.* (1984) shows however that this process can only contribute a maximum of 3 percent of the O_2 photodissociation. More recently, Frederick and Cicerone (1985) have indicated that, if the dissociation cross section of the excited $O_2(a^1\Delta g)$ molecule has a maximum value of order 10^{-19} cm^2, the process $O_2\ (a^1\Delta g) + h\nu \rightarrow O_2\ (c^3\Sigma_u) \rightarrow O(^3P) + O(^3P)$ has the potential to provide a substantial source of odd oxygen (comparable to the J_{O_2}source) in the upper stratosphere and mesosphere. This potential source appears to be ruled out, however, by recent laboratory measurements of absorption by $O_2\ (^1\Delta g)$ (Simonaitis and Leu, 1985); these data yield an upper limit for the cross section of 8×10^{-22} cm^2.

8.3 OZONE AND TEMPERATURE CORRELATIONS

In this section, developments concerning the two observational and theoretical relations between the ozone and temperature fields are reviewed. The analysis of such relations can broaden our view of the photochemistry and dynamics of the stratosphere and could prove useful in an attempt to understand the model ozone deficit (above 35 km) discussed in the previous section.

The dependence of chemical reaction rate constants upon temperature is the primary cause of the ozone sensitivity to temperature. When dynamics and chemistry are both important, one expects differing relationships between ozone and temperature perturbations as a function of height, whether these perturbations are spatial (e.g. longitudinal wave-like phenomena about zonal mean quantities) or temporal. The mechanistic model of Hartmann and Garcia (1979) showed that the eddy fields of velocity, temperature, and ozone mixing ratio associated with planetary wave disturbances exhibit characteristic phase relationships. In the lower stratosphere, where ozone can be regarded as an inert tracer, temperature and ozone perturbations are expected to be very nearly in phase, whereas a 180° phase shift is found in the upper stratosphere, where photochemistry should dominate over dynamics. A transition region exists in the middle stratosphere, where significant ozone transport can still be produced (see also Kawahira, 1982).

Such general relationships between local temperature and ozone fields have been deduced from various upper stratospheric satellite data for some time (Barnett *et al.*, 1975; Ghazi *et al.*, 1976; Ghazi and Barnett, 1980b; Krueger *et al.*, 1980; Gille *et al.*, 1980b; Wang *et al.*, 1983; Barth *et al.*, 1983; Miller *et al.*, 1984). Chandra (1985) has recently discussed the existence of an interesting global oscillation in ozone and temperature at 2 mbar (with period of 3-5 weeks) based on 2 years (1970-1982) of data from the Selective Chopper Radiometer (SCR) and Backscattered Ultraviolet (BUV) experiments on Nimbus 4. The Limb Infrared Monitor of the Stratosphere (LIMS) experiment also obtained strong evidence for the spatial and temporal anti-correlation between simultaneously measured ozone and temperature fields (Keating *et al.*, 1985; Froidevaux *et al.*, 1985b). Figures 8-11(a) through 8-11(c) were selected from the references mentioned above in order to display a variety of upper stratospheric situations where the out-of-phase relation between ozone and temperature has been observed. As shown in some of the above references, an in-phase relation at lower altitudes has also been observed.

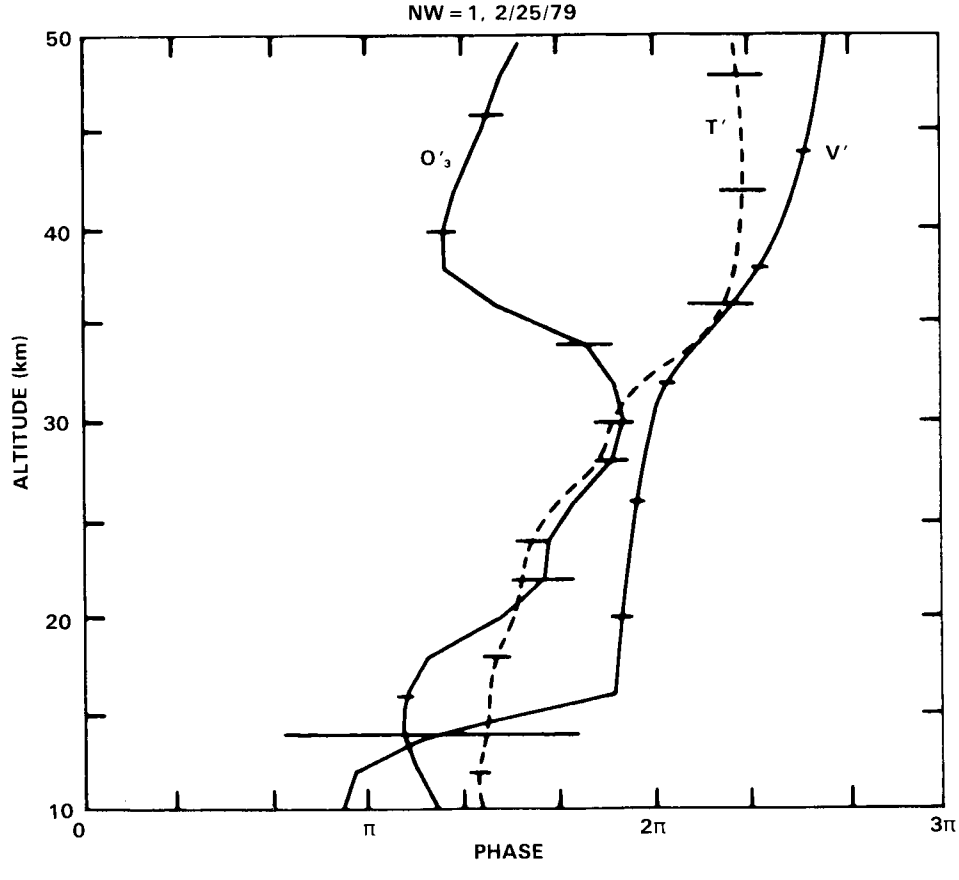

Figure 8-11.a Phase relationship between ozone (solid line), temperature (dashed line) and eddy meriodional velocity (solid and dashed line) waves (wave-number 1) during the late February 1979 warming. This figure is taken from an analysis of SAGE ozone data and meteorological information by Wang *et al.* (1983). The difference between an out-of-phase relationship between ozone and temperature in the upper stratosphere and in-phase relationship in the lower stratosphere is clearly seen.

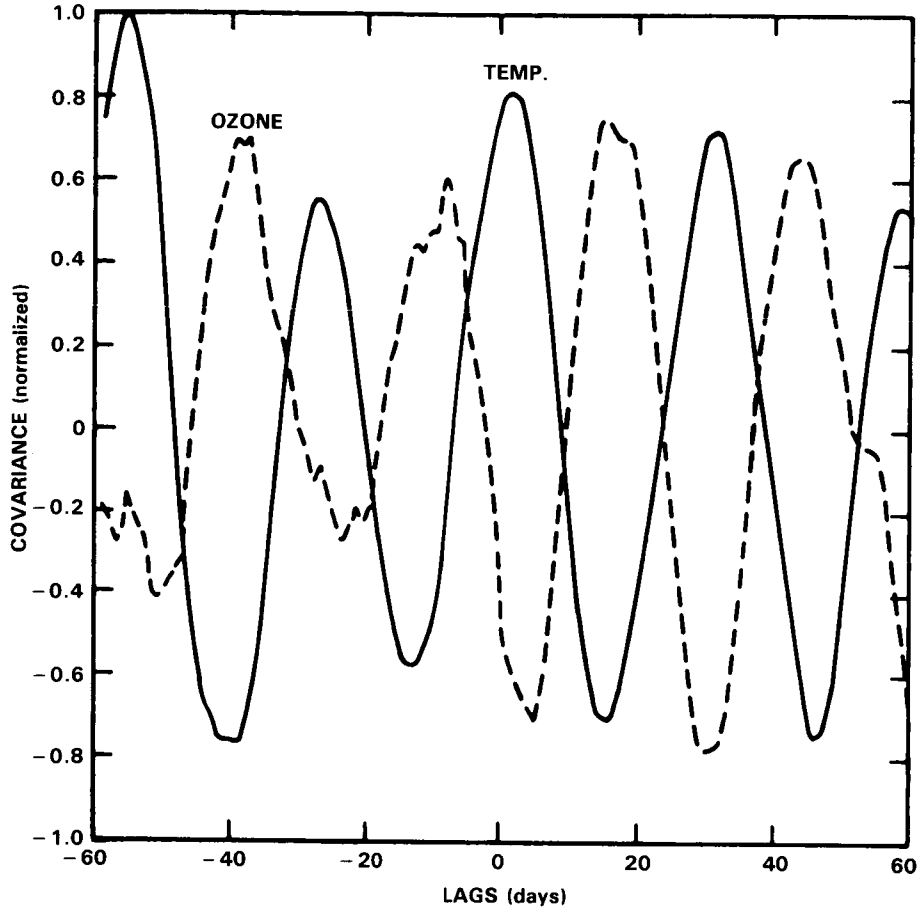

Figure 8-11.b Covariance of $F_{10.7}$ solar index and temperature and $F_{10.7}$ and ozone mixing ratio of 2 mbar in the tropics. This analysis (Chandra, 1985, see text for data sources) displays the anticorrelation between ozone and temperature fields as a function of time.

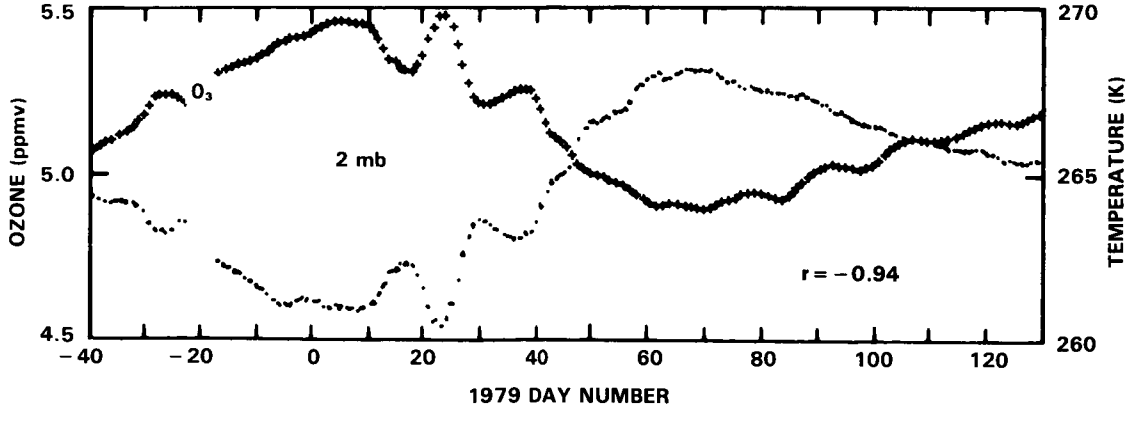

Figure 8-11.c Comparison between 5 day running means of O_3 (ppmv) and temperature (K) at 2 mbar as measured by Nimbus 7 LIMS. Data are zonal means averaged between 0° ± 20° latitude (from Keating *et al.*, 1985).

While the broad scheme depicted above (an upper stratospheric photochemical control of ozone with an associated out-of-phase relation between O_3 and T, and a lower stratospheric dynamical control with O_3 and T approximately in phase) might well hold for part of the globe during most seasons, one should be cautious not to blindly interpret observed phase relations in terms of "pure" photochemistry or "pure" dynamics. Indeed, Rood and Douglass (1985), Douglass *et al.* (1985), and Stolarski and Douglass (1985) have discussed this point by analyzing the individual terms (photochemical and dynamical) in the continuity equation for the perturbed fields of O_3 and T. This was done for both model and observational analyses, the latter case referring to winter satellite data from Nimbus 7 (SBUV ozone), NOAA 5 and Tiros-N (temperature). One conclusion from the above studies is that a strong anti-correlation between the O_3 and T eddy fields, coupled with a good agreement between the observed ozone perturbation and that deduced from photochemical equilibrium, does not necessarily imply that the individual dynamical terms are not important, compared to the photochemical terms (although the net dynamical contribution is small). In fact, the dynamically-induced phase differences between ozone and temperature waves can mimic the relationship expected from photochemical equilibrium. Moreover, dynamic forcing in the transition region can lead to a wide range of correlations between ozone and temperature perturbations.

The LIMS observations of ozone and temperature provide the best data available (simultaneous measurements with same instrument, good height resolution and observational precision) to quantitatively analyze ozone-temperature correlations. One way to do this is by evaluating the parameter $\theta = \partial 1n([O_3]/[M],/\partial(1/T)$ which relates to the ozone sensitivity to temperature changes. Expected values of θ can be algebraically estimated for individual cycles (O_x, HO_x, NO_x, or ClO_x), and approximate expressions for the combined chemistry can be obtained as well (Barnett *et al.*, 1975a; Haigh and Pyle, 1982). An illustration of the expected relative importance of the individual cycles as a function of height, as well as the combined result for all cycles together, is given in Figure 8-12, taken from the recent analysis of LIMS observations (mid-latitudes, May 1979) by Froidevaux *et al.* (1985b). These results come from an iterative algebraic solution to the odd oxygen photochemical balance equation, and include opacity feedback effects. The above study also reveals that there are regions of disagreement between the observed and theoretical values of θ particularly in the 3-5 mbar range, where model results are typically much higher (a factor of two) than the values inferred from LIMS data, even for statistically significant correlation coefficients between ozone and temperature. Uncertainties in the current chemistry or in the relative importance of the various cycles cannot account for these large differences, but dynamical contributions – as mentioned above – could play a role in this problem. The above authors also argue that short-term (less than a day) temperature fluctuations cannot be "tracked" by ozone in the middle and lower stratosphere, where its photochemical lifetime increases rapidly, and that such a phenomenon might be responsible for the disagreement in θ values (i.e., the lack of photochemical equilibrium). Frederick (1981) has discussed a similar effect in relation to the longitudinal phase differences between ozone and temperature fields. The value of θ itself, in addition to the correlation coefficient for O_3 and T, might serve as a useful diagnostic of the absence of photochemical equilibrium; its evaluation is more direct than the calculation of individual dynamical terms in the continuity equation. Agreement between the observed and predicted θ values, however, does not necessarily imply that dynamical terms are negligible and that photochemical control is strictly established. This could limit the usefulness of θ as a test of the model photochemistry.

Despite the interesting emerging analyses of ozone-temperature correlations, it does not appear that such analyses can readily lead to possible solutions to the significant model ozone deficit question raised in the previous section.

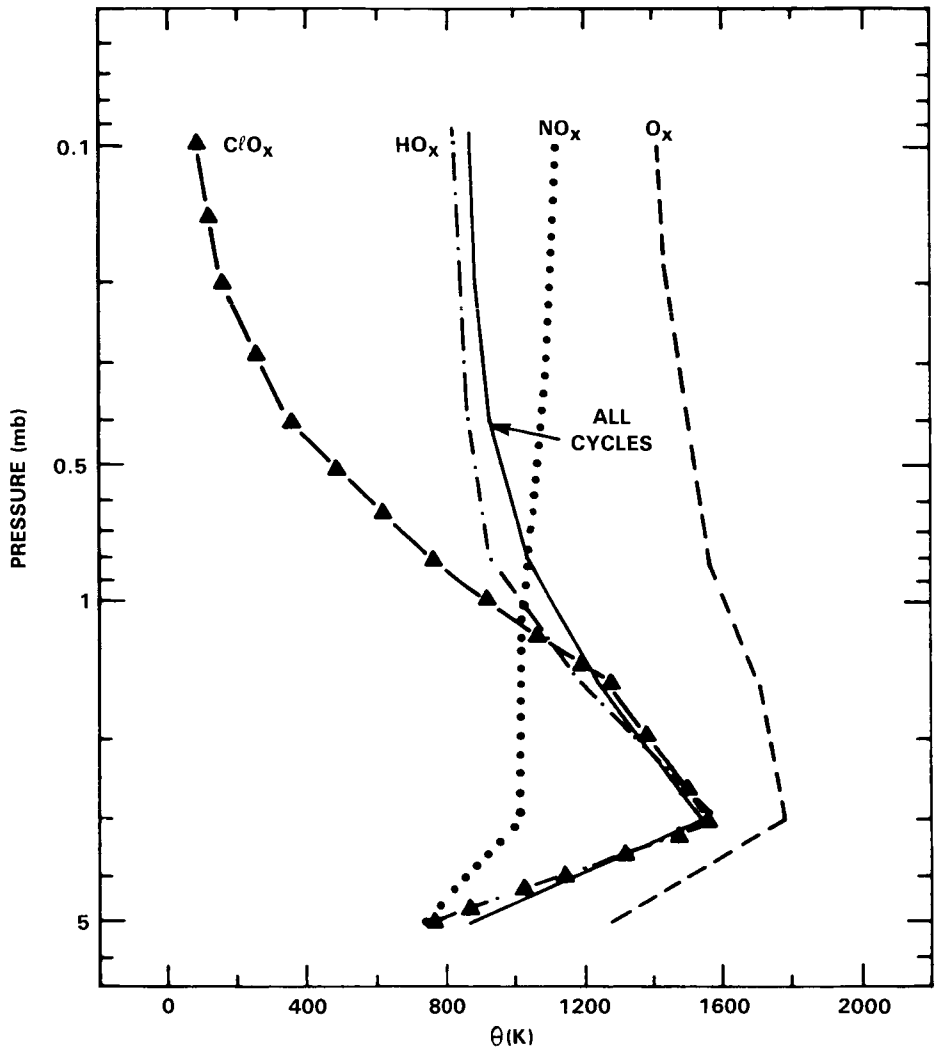

Figure 8-12. Theoretical estimate of sensitivity parameter θ (see text) in the upper stratosphere/lower mesosphere for individual chemical cycles (O_x, HO_x, NO_x and ClO_x) and all cycles combined. Model is for May 30°N and uses O_3, NO_2, H_2O and T data from LIMS (Froidevaux *et al.*, 1985b).

8.4 OZONE AND SOLAR VARIABILITY

Since the formation of ozone results from the photodissociation of molecular oxygen in the Herzberg continuum (stratosphere) and in the Schumann-Runge bands (mesosphere), one should expect slight changes in the O_3 mixing ratio with solar activity. As indicated in Chapter 6, the irradiance received at the earth is known to vary over a 27 day rotation of the Sun with typical values of 5 to 7 percent in the 175-210 nm region, 3 percent between 210 and 250 nm and 1 percent or less beyond 260 nm.

Analyses of the ozone response to short term solar variability have been reported recently by Hood (1984), Gille *et al.* (1984c), Chandra (1985) and Keating *et al.* (1985). These are based on different methods and on data from various sources. It might be interesting to briefly review these studies in order to see if their conclusions are in accord with the model predictions.

Hood (1984) has used the Nimbus 4 BUV ozone measurements (Fleig *et al.*, 1981) to estimate the response of upper stratospheric O_3 to UV changes. Since, at these heights, the temperature is negatively correlated with ozone (see Section 8.4), this endogenic component of the O_3 variation has been removed approximately by using a photochemical model in which the temperature was modified as a function of time according to the measurements by the Nimbus 4 Selective Chopper Radiometer. The residual ozone mixing ratio at low latitude was found to contain short term variations positively correlated with variations in the radiometric 10.7 cm flux and in the 180-190 nm UV flux as determined by the model of Lean *et al.* (1982) based on ground-based Ca II K line measurements.

Chandra (1985), however, using the same data as Hood (1984) showed that the oscillations in tropical ozone and temperature are apparently related to higher latitude waves and that the observed variability in ozone near the equator should probably be attributed to planetary waves rather than solar UV oscillations.

Using a statistical spectral method to treat ozone distributions reported by the LIMS instrument and solar irradiances measured by the SBUV experiment, both on board Nimbus 7, Gille *et al.* (1984c) have found that the ratio of the percentage O_3 response in the tropics to the percentage UV change at 205 nm increases with altitude from 0.17 at 30 km to 0.38 at 54 km reaching probably 0.60 at 60 km (see Figure 8-13). Keating *et al.* (1985), adopting data from the same source, have corrected for temperature

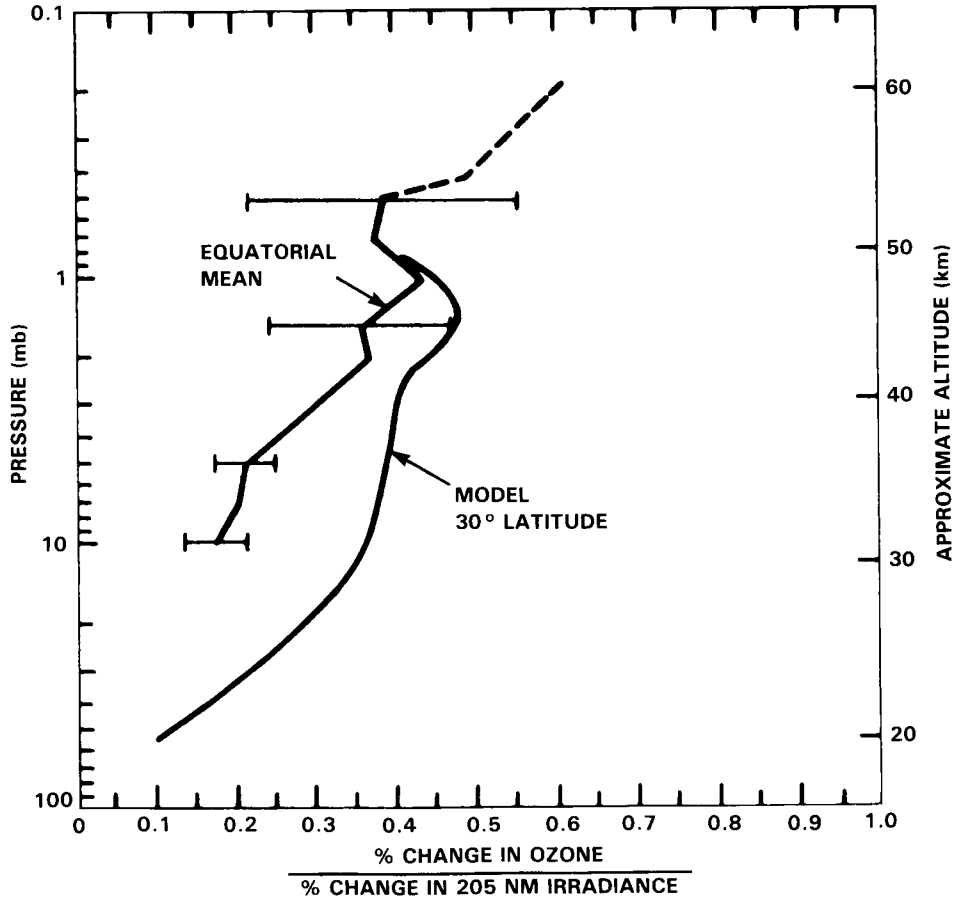

Figure 8-13. Sensitivity of the ozone concentration to a 1% change in the UV irradiance at 205 nm. Values derived from the LIMS and SBUV data compared with a model simulation (Gille et al.,1984c).

variations by making use of the temperature data measured simultaneously by LIMS to derive at each level a relation between temperature and ozone variations. This method allows to extract endogenic effects due to dynamics and in particular to planetary waves. The small residual variations can be attributed to exogenic solar influence since they correlate strongly with the variability in the measured solar irradiance at 205 nm (Figure 8-14). The percentage change in ozone relative to the percentage change in the UV flux at 205 nm is estimated to be of the order of 0.3 between 5 and 0.5 mbar, and to increase significantly above the stratopause. These results as well as those of Gille *et al.* (1984c), are in reasonable agreement with theoretical model predictions below about 40-50 km. Above this level, the predicted sensitivity of ozone to UV is considerably lower than the sensitivity inferred from the data. This discrepancy is consistent with the ozone imbalance discussed previously since it could be resolved by reducing the effect of odd hydrogen on the odd oxygen loss or by increasing the contribution of short wave radiation to the O_3 production.

Solar induced modifications of the ozone layer in relation with the 11 year solar cycle have been recently studied by Natarajan *et al.* (1980/81), Brasseur and Simon (1981) and Garcia *et al.* (1984). Some of this work as well as previous studies have been reviewed by Keating *et al.* (1981). Moreover, an analysis of 7 years of Nimbus 4 BUV data by Chandra (1984) has shown that the globally-averaged ozone in the upper stratosphere, when corrected for instrument drift, decreased by 3 to 4 percent from 1970 (solar maximum) to 1976 (solar minimum).

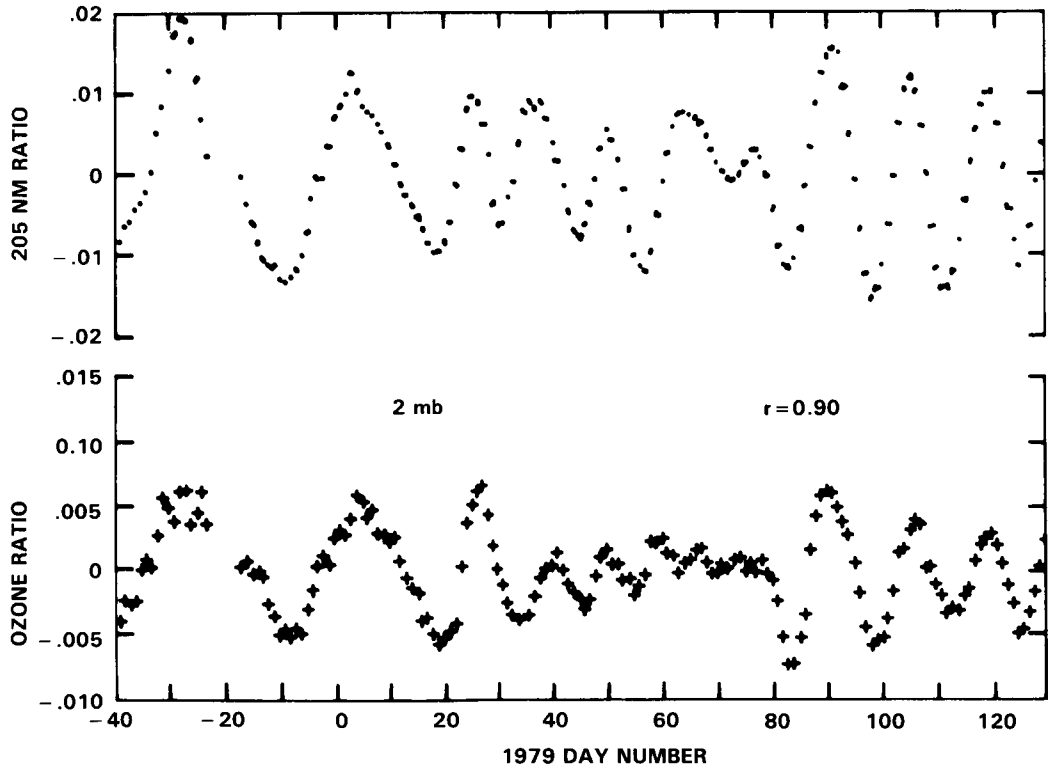

Figure 8-14. Relation between relative variation in the ozone mixing ratio (lower curve) and in the solar UV irradiance at 205 nm (upper curve) at 2 mbar after correcting for temperature effect. The ozone values refer to a zonal mean averaged over ± 40° latitude (from Keating *et al.*, 1985).

The recent model of Garcia *et al.* (1984), based on the model by Lean *et al.* (1982) for solar variability at wavelengths shorter than 200 nm, shows, from solar minimum to solar maximum, an increase in the ozone concentration of less than 5 percent in the stratosphere but considerably higher in the upper mesosphere and lower thermosphere (Figure 8-15). The reduction predicted in the lower mesosphere is attributed mostly to the increase in the dissociation of water vapor and the resulting increase in the HO_x-catalyzed ozone destruction. The negative change computed at high latitude near the stratopause reflects the increase in odd nitrogen as a result of higher production of NO_x in the thermosphere and its downward transport near the polar region. These predicted changes should be considered as upper limits since the model by Lean *et al.*, predicts higher solar variability than inferred directly from the SME data (see Chapter 7).

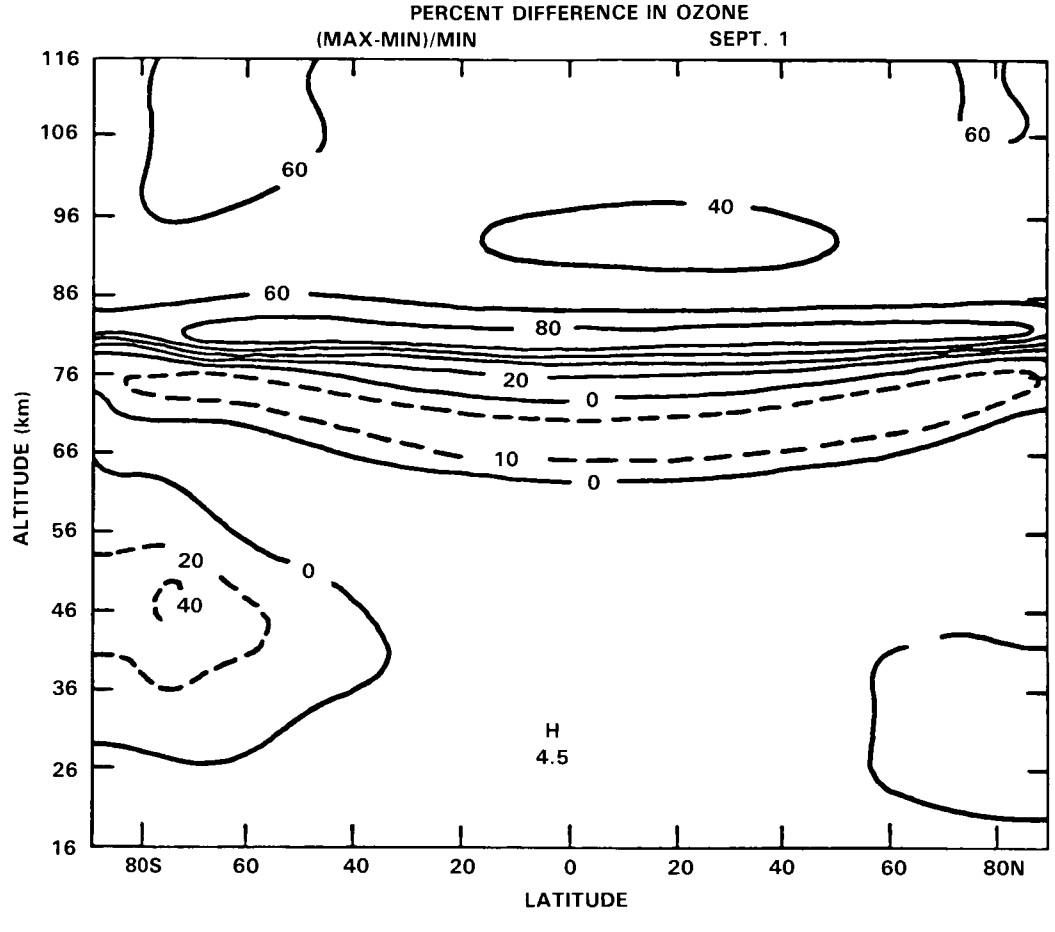

Figure 8-15. Ozone density variation over the course of the 11 year cycle of solar activity as calculated by Garcia *et al.* (1984).

From these studies, one may conclude that most of the short-term ozone variations observed on a global scale even in the tropics, are related to planetary wave activity but that a refined treatment of the data can reveal small oscillations induced by variations in the solar output. It is estimated that a 5-6 percent change in the solar irradiance at 205 nm over a solar rotation period (27 days) leads to a fluctuation in mid and upper stratospheric ozone on the order of 2-3 percent. No detectable change in the ozone column should be expected.

Ozone also responds to long-term variations in the solar output related to the 11-year cycle. The corresponding change in mid-stratospheric ozone is expected to be less than 5 percent and the variation of the ozone column should be of the order of 1 to 3 percent.

8.5 OZONE AND SOLAR PROTON EVENTS

Particle precipitation events (generally high latitude solar proton events or SPEs) have been studied intensively mostly during the last few years. Very few such studies had been published much prior to the 1981 WMO Report. The interest in these events stems from the opportunity that they provide for analyses of the perturbed middle atmosphere in a kind of "natural laboratory" experiment. Our understanding of the complex interactions affecting ozone can be tested and furthered by studying simultaneous observations of particle precipitation events and related changes in the ozone abundance.

Since the initial evidence of ozone changes resulting from an SPE reported by Weeks *et al.* (1972), based on rocket measurements between 50 and 70 km, analyses of ozone satellite data from the Nimbus 4 BUV experiment (Heath *et al.*, 1977; Fabian *et al.*, 1979; Reagan *et al.*, 1981; McPeters *et al.*, 1981; Solomon and Crutzen, 1981; Rusch *et al.*, 1981), the Nimbus 7 SBUV experiment (McPeters and Jackman, 1985; Jackman and McPeters, 1985), and the Solar Mesosphere Explorer (Thomas *et al.*, 1983b; Solomon *et al.*, 1983b) have all produced qualitatively similar correlations between SPEs and ozone. Nine such events have now led to identifiable ozone depletions.

The theoretical interpretation relies on HO_x or NO_x related catalytic destruction of ozone. The added HO_x or NO_x radicals (in the models) are products that follow the degradation of primary particles, dissociative and ionizing effects of secondary electrons on N_2, O_2, and other species, and subsequent neutral and ion chemistry in the middle atmosphere (Swider and Keneshea, 1973; Crutzen *et al.*, 1975; Frederick, 1976; Swider *et al.*, 1978; Crutzen and Solomon, 1980; Rusch *et al.*, 1981; Solomon *et al.*, 1981). Both short-term (1 day or less) and long-term (1 week or more) ozone responses have been observed, these responses being understood as a product of HO_x (short-lived) and NO_x (long-lived) related chemistry, respectively. It is expected that the HO_x radicals will be mostly responsible for ozone changes above the stratopause, while NO_x production effects become important mostly below that level. Model and observational results for ozone depletions at heights between 60 and 85 km agree reasonably well. Below 45 km, the observed ozone decrease associated with the large SPE that occurred on August 4, 1972, follows approximately the predicted response. Also, one expects a relative increase in the ozone depletion as the solar zenith angle increases, due to the increased importance of the SPE HO_x source (independent of solar zenith angle), relative to the (angle-dependent) natural source from H_2O. Such an effect has been analyzed in a few cases (Solomon *et al.*, 1983b see Figure 8-16; Jackman and McPeters, 1985), and the observed relative ozone decrease with solar zenith angle appears to be fairly well represented by the above explanation.

Despite these encouraging results, McPeters *et al.* (1981) and Jackman and McPeters (1985) have pointed out that some ozone depletions observed between 50 and 60 km are significantly larger than the predicted values. Results from a totally self-consistent calculation are in much worse disagreement with observations than calculations using observed ozone depletions to determine relevant values of the radiation field as a function of height. In either case, it is difficult to account for the observed ozone depletions, even if model parameters are allowed to vary within reasonable bounds. Whether this problem is due to an incomplete understanding of the HO_x-related chemistry, to uncertainties in the absorption cross sections for O_2 or O_3, or to some other reason remains to be seen.

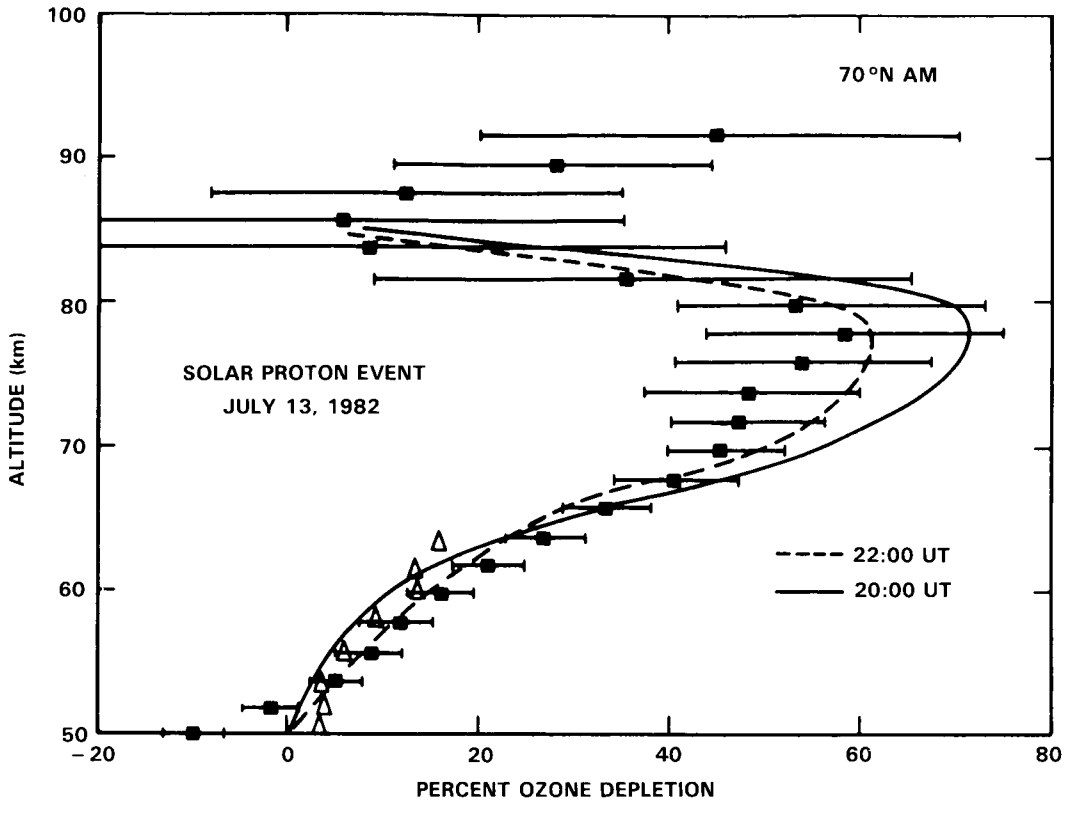

Figure 8-16. Observed and calculated ozone depletion during the solar proton event of July 13, 1982 (from Solomon *et al.*, 1983b).

The solution to this problem could be related to the ozone balance problem above 35 km. This should provide additional motivation for closely studying relationships between particle precipitation events and the ozone abundance near the stratopause.

8.6 OZONE VARIATIONS ASSOCIATED WITH EL CHICHON/EL NINO

Within Chapter 14 discussion is presented on the extended total ozone minimum observed during the winter of 1982-1983 and referred to as the "ozone hole," Figure 14-2. The timing of this phenomenon has been related to either or both of two separate events; the volcanic eruption of El Chichon in March-April of 1982 and the large atmospheric circulation anomalies associated with the El Nino of this time period.

With respect to the El Chichon, the arguments suggestive of a volcanic association have been presented by Dütsch (1985) and Vupputuri (1985). An ozone decrease on the order of 10 percent is observed between 100 and 30 mbar from ozone balloonsonde data that is connected through its timing and attributes to the El Chichon event. Two possible mechanisms were proposed; aerosol heterogeneous chemistry and direct chlorine injection.

Quiroz (1983 a,b) and Angell *et al.* (1985), on the other hand, point out that the '82-83' period was, coincidentally, that of a major El Nino event which has been associated with extraordinary climatic anomalies in the troposphere. Quiroz (1983a) has specifically demonstrated the difficulty of separating the stratospheric temperature signal from the two events and it is clear that considerable work must be done for the ozone data.

8.7 SUMMARY AND SUGGESTIONS FOR FUTURE RESEARCH

In this chapter, questions related to odd oxygen have dealt primarily with the photochemically dominated altitude region, i.e. the upper stratosphere and lower mesosphere. The absolute abundance of ozone and relationships between ozone and imposed variations in atmospheric temperature, solar UV flux and solar proton precipitation are being studied with the help of an increasingly accurate and large data base (from spaceborne experiments in particular), and increasingly accurate models of the middle atmosphere. From the analyses carried out in the last few years, several possibly related problems appear to exist in our understanding of the region above about 35 km.

Comparisons of SBUV, LIMS and SAGE profiles for April 1979 indicate a standard deviation of about 15% from 25-30 km which decreases to about 6% from 30-55 km. As these three instruments use such different techniques, these values represent our ability to measure the ozone profile in an absolute sense. These values are within the root mean square systematic error summaries. In the lower levels where the satellite data overlap with the ozone balloonsondes there is more ambiguity, but it appears that the balloonsondes are systematically lower than SBUV above about 32 km. The cause of this pattern is not currently recognized.

Utilizing SBUV as the basic data source for four year zonal average profiles, the random uncertainties appear to be about 4% in mid- and high-latitude winter and about 2% elsewhere.

The observed ozone abundance above 35 km is significantly underestimated by model calculations. This model deficit is typically 30-50%, and in some cases is as large as a factor of two. This ozone imbalance can only marginally be accepted as being due to the combined errors in the models and observations. It is not clear which of the possible solutions (underestimate of the model O_x production rate, overestimate of the model O_x loss rate, or missing chemistry) is most likely at present. Suggestions for future research include: a) Laboratory work to reduce the model uncertainties in key photochemical parameters, in particular HO_x radical chemistry and absorption cross sections for O_2 (Schumann-Runge bands and Herzberg continuum) and O_3 ($O(^1D)$ channel); b) Stratospheric measurements relating to the above cross section determinations (i.e., high resolution solar flux data within as large an altitude range as possible, from 180 to 250 nm); c) better understanding of the local ozone photochemical balance in the upper stratosphere (i.e., simultaneous measurements of the key radical species involved). However a quantitatively accurate observational determination of the O_3 balance is not possible, due to the importance of the local dynamics and since the required accuracy in the measurements of the individual parameters cannot yet be achieved; d) Precise measurements of the $[O]/[O_3]$ ratio; e) A search for possible additional production mechanisms; f) Measurement and detailed consideration of the diurnal waveform of O_3 as a means of testing photochemistry in the upper stratosphere; g) Continued use of models to test the expected ozone sensitivity to newly arising recommendations of photochemical parameters; h) More detailed analyses of radiative and dynamical effects on ozone with the use of observations as well as multidimensional models.

In addition, comparisons of theoretical and observed relationships between ozone and temperature, ozone and solar UV, and ozone and solar proton events reveal a number of discrepancies which require further analyses.

The problems discussed in the present chapter, in particular the significant ozone imbalance in the photochemically-controlled region of the middle atmosphere, limit the confidence that can be attached to model predictions of future ozone changes in response to long-term increases in the emission or source gases.

With respect to requirements for future effort, we also recommend the following:

1. Resolve the causes of the ozone measurement biases between SBUV, LIMS, SAGE as well as balloonsondes and, thereby, reduce the absolute error estimates.

2. Determine the impact of implementation of the Bass and Paur ozone absorption coefficients in the ground based measurements and compare the results with satellite observations.

3. Continue development of the ground based profile measurement program with particular emphasis on the following:

   a. Determination of the El Chichon aerosol impact on Umkehr measurements.
   b. Development of the high altitude (about 40 km) balloon sampling system with specific attention to the adjustment procedure to match the Dobson total ozone measurement.
   c. Development of a Lidar system capable of routine ozone and temperature measurements in the troposphere and stratosphere, especially above about 40 km.